Copernicus
Europe's eyes on Earth

Copernicus Atmosphere Monitoring Service

Upgrade verification note for the CAMS near-real time global atmospheric composition service

Evaluation of the e-suite experiment gu42

Issued by: KNMI

Date: 6-3-2018

Ref: CAMS84_2015SC3_D84.3.1.5_201802_esuite_v1

IMPLEMENTED BY
ECMWF

Copernicus
Europe's eyes on Earth

Upgrade verification note for the CAMS near-real time global atmospheric composition service

Evaluation of the e-suite experiment gu42

AUTHORS:
S. BASART (BSC), A. BENEDICTOW (METNO), Y. BENNOUNA (CNRS-LA),
A.-M. BLECHSCHMIDT (IUP-UB), S. CHABRILLAT (BIRA-IASB),
Y. CHRISTOPHE (BIRA-IASB), H. CLARK (CNRS-LA), E. CUEVAS (AEMET),
H. ESKES (KNMI), K. M. HANSEN (AU), U. IM (AU), J. KAPSOMENAKIS (AA),
B. LANGEROCK (BIRA-IASB), K. PETERSEN (MPG), M. SCHULZ (METNO),
A. WAGNER (MPG), C. ZEREFOS (AA)

REPORT OF THE COPERNICUS ATMOSPHERE MONITORING SERVICE, VALIDATION SUBPROJECT.

STATUS:
VERSION 1, FINAL

DATE:
6/3/2018

Executive Summary

The Copernicus Atmosphere Monitoring Service (CAMS, http://atmosphere.copernicus.eu) is a component of the European Earth Observation programme Copernicus. The CAMS global near-real time (NRT) service provides daily analyses and forecasts of reactive trace gases, greenhouse gases and aerosol concentrations.

CAMS has a sub-project (CAMS-84) dedicated to the validation of the service products. The validation results for the CAMS global NRT service (the o-suite) products and high-resolution greenhouse gas simulations can be found in Eskes et al. (2018) and Eskes et al. (2015). The observational datasets used for this validation are described in Douros et al. (2017). These validation reports and the verification websites can be found here: http://atmosphere.copernicus.eu/user-support/validation/verification-global-services.

This document contains an evaluation of the upgrade of the NRT service planned in the first half of 2018. Before the upgrade, the new model configuration (the e-suite) is operated in parallel to the operational NRT service (the o-suite) for about half a year. Below the main results are summarised from a comparison of the performance of the forecasts with the new e-suite run (experiment id "gu42", period July 2017 - January 2018), the operational run (o-suite) and independent observations.

Noteable changes between this e-suite and the operational o-suite are updates in the sea-salt and dry deposition modelling of aerosols. Section 1 provides a brief overview of the model changes between the e-suite and o-suite. Section 2 contains the figures that provide the evidence for the conclusions presented below.

Main conclusions

The candidate model configuration shows significant differences compared to the o-suite as far as aerosols is concerned. Changes in sea salt results in positive biases. Overall the quality of the e-suite aerosol distribution, including dust, is similar or slightly worse than the o-suite. Tropospheric ozone e-suite and o-suite results generally are very comparable, apart from a reduction in ozone over Antarctica as compared to the current operational version. Stratospheric ozone is very similar as compared to the present operational version. The other trace gas concentrations (CO, NO2, HCHO, methane) also show only minor differences.

Global Aerosol

Taking the o-suite from September to November 2017 as reference, the following changes wrt to aerosol optical depth (AOD) can be found in the e-suite: AOD increases (+13%) are seen mainly due to sea salt increases (Table 2.1.1). Consequently, a larger bias is found for AOD against Aeronet sun photometers (Fig. 2.1.3, 2.1.4). The quality of the IFS e-suite, despite or because of the significant shift in the aerosol composition is slightly worse than the o-suite. The Angström exponent, reflecting aerosol size, was slightly worse (Fig. 2.1.5). There is still a 16% AOD loss in the first 3 days

of forecast indicating an initial day imbalance between emissions and removal introduced by the assimilation.

Dust

Summary of the results for dust are the following:

- DOD in the NAMEE Region (Table 2.1.3): Both CAMS experiments show similar results which are comparable with the SDS-WAS Multi-model.

- AOD in the NAMEE Region (Table 2.1.5): In general, the e-suite shows a higher overestimation with mean bias values of 0.05 (o-suite 0.03) on average for all the AERONET sites. The e-suite shows better results in the Mediterranean and the Middle East than o-suite regarding correlation, but lower correlation values in the Sahel and Tropical North Atlantic.

Aerosol validation over the Mediterranean

AOD in the Mediterranean (e.g. Fig. 2.1.6): The e-suite shows higher background levels than the o-suite which are not associated with natural aerosols (i.e. sea-salt and dust).

PM in the Mediterranean (e.g. Fig. 2.1.7): The maximum PM10 and PM2.5 levels simulated by the e-suite present differences with respect o-suite in maritime sites such as Venaco. These maximum PM10 and PM2.5 peaks are linked to sea-salt contribution. This is because the e-suite includes changes in the sea-salt component (new sea-salt emission scheme). A bug in the sedimentation speed for sea-salt has been corrected in the new o-suite (from 26-Sep-2017), but the new sea-salt emission scheme included in the e-suite seems more important than the correction of the bug.

Tropospheric ozone (O$_3$)

Model profiles of the CAMS runs were compared to free tropospheric balloon sonde measurement data (see Fig. 2.2.1, 2.2.2). Small differences between the o-suite and the e-suite show in all regions, but the largest deviations in MNMBs show over Antarctica, where the e-suite has larger negative MNMBs (o-suite: between -6 and 4%, e-suite between -19 and -6%). Note that only few soundings have been available for this period. Over the northern Midlatitudes and the Arctic, the e-suite has lower MNMBs than the o-suite (northern Midlatitudes: e-suite: 0 to-3% , o-suite: 3-6%; Arctic: e-suite: 5-12% , o-suite: 8-16%). Over the Tropics, MNMBs for the two runs are nearly identical.

For the Near Real Time (NRT) validation, 12 GAW stations and 13 ESRL stations are currently delivering O$_3$ surface concentrations in NRT, and the data are compared to model results between June-August 2017 (Fig. 2.2.3 to 2.2.5) for GAW, and May-November 2017 for ESRL (Fig. 2.2.6 and 2.2.7). At the surface the e-suite shows lower MNMBs for European and Asian GAW stations (Europe e-suite: between -1 and 9%, o-suite: 4-12%; Asia e-suite: between 32 and 61%, o-suite: 33-63%). Larger negative MNMBs appear for stations in the Southern Hemisphere (e-suite: -4 to -19%, o-suite: -12% to 4%). Correlation coefficients are mostly identical.

At ESRL stations in general there are only small differences for surface ozone between e- and o-suite. For the majority of stations the e-suite has slightly lower MNMBs compared to o-suite (about 0% - 3%) and about equal correlations (Fig. 2.2.6 and 2.2.7). The only exception is Antarctica where

o-suite seems to perform better than e-suite in terms of correlations. This could be related to the last o-suite upgrade (during September) which may cause a virtual effect in the o-suite seasonality.

Compared to IAGOS aircraft profiles, the e-suite behaves very similarly to the o-suite (Figs. 2.2.8-2.2.11). Ozone is always overestimated in the UTLS and the best comparisons with IAGOS are found in the free troposphere.

Tropospheric ozone (O₃) in the Mediterranean

In general the e-suite simulated O_3 surface ozone concentration are about 1.0-3.0 ppb lower than o-suite O_3 surface ozone concentration in the Mediterranean area. Thus e-suite biases are slightly less positive/slightly more negative than o-suite, and in most cases the o-suite performs slightly better than the o-suite. On the other hand, for the majority of Mediterranean stations used in the current report, the e-suite correlation coefficients are slightly higher than for the o-suite (Table 2.2.1, Figure 2.2.12).

Tropospheric ozone (O₃) in the Arctic

Surface ozone measurements from Arctic sites were applied to evaluate the e-suite against the o-suite. There are no large differences in the performance of the e-suite and the o-suite for surface ozone at Svalbard, Tiksi and VRS in the Arctic for May – December 2017. The variability of the e-suite is lower, especially for high peak concentrations predicted at Tiksi (Fig. 2.2.13), which is in better agreement with observations than the o-suite. The correlation coefficient of the e-suite run is higher than for the o-suite (between 0.03 and 0.08 higher).

Tropospheric Carbon Monoxide (CO)

Carbon monoxide surface concentrations have been compared with WMO Global Atmosphere Watch observations. For most stations the o-suite and e-suite show a similar behaviour (Fig. 2.3.1-2.3.3). Larger MNMBs are produced by the e-suite for Cape Verde station (e-suite: 14%, o-suite: 8%) and Minamitorishima station (e-suite: -10%, o-suite: -6%). Larger differences in correlation are found for Cape Verde (e-suite: 0.48, o-suite: 0.38) and Minamitorishima (e-suite: 0.69, o-suite: 0.8) stations.

The time-series of ozone at Paris compared to IAGOS aircraft observations (Fig.2.3.4 - 2.3.7) shows that the e-suite and o-suite are almost identical. Monthly-mean profiles in figure 2.3.5 again show that there is virtually no difference between the two runs.

CO total columns from o-suite and e-suite CAMS simulations are compared with MOPITTv7 and IASI for different regions from May until October 2017. There is nearly no differences between o-suite and e-suite in CO total columns (Fig. 2.3.8, 2.3.9). The model simulations reproduce well the CO total columns observed from MOPITT-v7 (within 5 %, apart for Alaska: within 10%), while IASI total columns show slightly higher CO total columns in Alaska Fire regions and Siberian Fire region and in North and South African Regions compared to MOPITTv7 and the model simulations. Comparison for the day 2 and day 4 forecasts show very little differences (Fig. 2.3.10). Figure 2.3.10 shows the CO total columns of MOPITTv7 and e-suite for June 2017, as well as the difference plot between o-suite and e-suite, and the differences between e-suite d0, d2 and d4 and MOPITTv7 for June 2017.

Tropospheric Nitrogen dioxide (NO$_2$)

The e-suite and o-suite perform very similar for comparisons against tropospheric NO$_2$ from GOME-2, there are only small differences between both model runs. Time series in Figure 2.4.1 show that e-suite and o-suite tend to overestimate the seasonal cycle over South Africa, underestimate the seasonal cycle over Europe and overestimate summer to autumn values over East-Asia compared to GOME-2. It is not clear if the ups and downs of wintertime GOME-2 values over Europe are realistic, although a quick inspection of daily GOME-2 satellite images in the last report did not point to problems regarding the retrieval. Gobal maps of tropospheric NO$_2$ for January 2018 (Figure 2.4.2) show that e-suite and o-suite strongly underestimate wintertime values over European anthropogenic emission areas and that shipping routes are more pronounced compared to GOME-2. (Most of these issues are known in general from previous NRT reports)

Formaldehyde (HCHO)

There is almost no difference between e-suite and o-suite, no major issues are found.

Model results and observations are in reasonable agreement for HCHO columns with respect to magnitude for time series shown in Figure 2.5.1. The models overestimate the seasonal cycle over East-Asia and tend to overestimate summertime values over Eastern-US. Negative values over Eastern US for GOME-2 and peak value in December are likely the result of a lack of satellite data (caused by instrument degradation) for this region during Northern Hemisphere winter months (see Figure 2.5.2 for an example). Global maps of tropospheric HCHO for January 2018 (Figure 2.5.2) show a rather good agreement between models and GOME-2, but both runs overestimate values over some parts of Australia and over forest fire regions in Central Africa.

Comparisons with NDACC MAX-DOAS observations at La Reunion indicates an increased negative bias in the e-suite compared to o-suite (Fig. 2.5.3).

Methane

Compared to NDACC FTIR, the negative methane bias is reduced in the e-suite and now (just) falls within the measurement uncertainty. The diference between the o-suite and e-suite seems to vanish near the end of 2017, see Fig. 2.8.1.

Stratospheric ozone

There is no significant difference between o-suite and e-suite compared to ozone sondes (Fig. 2.6.1 and 2.6.2) and satellite observations (MLS, OMPS-LP and ACEFTS) with respect to stratospheric ozone, both for the analyses and the 4th day forecast (96h to 120h).

Also when compared to satellite observations (MLS, OMPS-LP and ACEFTS, see Fig 2.6.3 and 2.6.4) in the pressure range of 1hPa to 100hPa, e-suite and o-suite are very comparable.

NDACC Microwave observations at Mauna Loa indicate an improvement (lower positive bias) in stratospheric ozone in the e-suite. At La Reunion the ozone concentrations are very comparable (Fig. 2.6.5).

Stratospheric Nitrogen dioxide (NO$_2$)

Stratospheric chemistry is not implemented in CIFS and hence models are not expected to show reasonable results for stratospheric NO_2. However, apart from a general understimation, the following may be interesting to note (Fig. 2.7.1): The e-suite shows an opposite trend than GOME-2 at northern latitude bands, where the trend of o-suite values agrees better with the satellite observations. The o-suite shows an opposite trend than GOME-2 at southern latitude bands since Sep 2017, where the trend of e-suite values agrees better with the satellite observations.

Table of Contents

1. Description of the o-suite and e-suite

Below a short model description is given on both the CAMS o-suite operational data-assimilation and forecast run and the new e-suite.

1.1 o-suite

The o-suite consists of the C-IFS-CB05 chemistry combined with the CAMS bulk aerosol model. The chemistry is described in Flemming et al. (2015), aerosol is described by the bulk aerosol scheme (Morcrette et al., 2009). Dissemination of the CAMS o-suite forecasts is two 5-day forecasts per day, based on 00UTC and 12UTC analyses. The o-suite data is also stored under expver "0001" of class "MC" of the MARS archiving system of ECMWF. The latest update of the o-suite occured on 26 September 2017. Information on the model versions can be found at http://atmosphere.copernicus.eu/user-support/operational-info .

Here a summary of the main specifications of this version of the o-suite is given:

- The meteorological model is based on IFS version CY43R1; the model resolution is T511 (approx. 40 km) with 60 vertical layers.

- The CB05 tropospheric chemistry is used (Williams et al., 2013), originally taken from the TM5 chemistry transport model (Huijnen et al., 2010)

- Stratospheric ozone during the forecast is computed from the Cariolle scheme (Cariolle and Teyssèdre, 2007) as already available in IFS, while stratospheric NOx is constrained through a climatological ratio of HNO3/O3 at 10 hPa.

- Monthly mean dry deposition velocities are based on the SUMO model provided by the MOCAGE team, with a resolution of 1.0×1.0 degree.

- The aerosol model includes 12 prognostic variables, which are 3 bins for sea salt and desert dust, hydrophobic and hydrophilic organic matter and black carbon, sulphate aerosols and its precursor trace gas SO_2 (Morcrette et al., 2009).

- Data assimilation is described in Inness et al. (2015) and Benedetti et al. (2009) for chemical trace gases and aerosol, respectively. A variational bias correction is used (Dee and Uppala, 2009). The data sets assimilated can be found in Table 1.1.

- Year-specific anthropogenic emissions are based on the MACCity emissions (Granier et al., 2011). Biogenic emissions originate from POET. Only for isoprene, a climatology of the MEGAN-MACC emission inventory (Sindelarova et al., 2014) is adopted. Resolution of emissions is 0.5×0.5 degree.

- NRT fire emissions are taken from GFASv1.2 (Kaiser et al. 2012), both for gas-phase and aerosol, available on 0.1×0.1 degree.

- Since 21 June 2016, two 5-day forecasts are produced per day (instead of one), based on 00UTC and 12UTC analyses. The 12UTC forecast will be available before 22UTC.

- Since 21 June 2016 there is a shift in the data assimilation windows from 9UTC-21UTC to 3UTC-15UTC, and from 21UTC-9UTC to 15UTC-3UTC.

Before 3 September 2015 the o-suite used an older meteorological cycle (CY40r2) and run under experiment (EXPVER) "g4e2". Before 18 September 2014 the o-suite was based on the coupled IFS-MOZART system (Stein et al., 2013), running under expid "fnyp".

Table 1.1: Satellite retrievals of reactive gases and aerosol optical depth that are actively assimilated in the o-suite.

Instrument	Satellite	Provider	Version	Type	Status
MLS	AURA	NASA	V3.4	O3 Profiles	20130107 -
OMI	AURA	NASA	V883	O3 Total column	20090901 -
GOME-2A	Metop-A	Eumetsat	GDP 4.7	O3 Total column	20131007 -
GOME-2B	Metop-B	Eumetsat	GDP 4.7	O3 Total column	20140512 -
SBUV-2	NOAA	NOAA	V8	O3 21 layer profiles	20121007 -
IASI	MetOp-A	LATMOS/ULB	-	CO Total column	20090901 -
IASI	MetOp-B	LATMOS/ULB	-	CO Total column	20140918 -
MOPITT	TERRA	NCAR	V5-TIR	CO Total column	20130129-
OMI	AURA	KNMI	DOMINO V2.0	NO2 Tropospheric column	20120705 -
OMI	AURA	NASA	v003	SO2 Tropospheric column	20120705-20150901
GOME-2A/2B	METOP A/B	Eumetsat	GDP 4.7	SO2 Tropospheric column	20150902-
MODIS	AQUA / TERRA	NASA	Col. 5 Deep Blue	Aerosol total optical depth	20090901 - 20150902 -
OMPS	Suomi-NPP	NOAA / EUMETSAT		O3 profile	
PMAp	METOP A METOP B	EUMETSAT		AOD	20170124 - 20170926 -

1.2 e-suite

The CAMS NRT research e-suite for CY45R1_CAMS (experiment **gu42,** class **rd**) was started on 2017-11-15 for the analysis cycle 2017050100. This e-suite runs at T511L60.

Main features (with new items in italics) are:

- 120 h long forecast from 00UTC and 12UTC

- IFS cycle 45R1

- IFS-TM5

- MACCity anthropogenic emissions

- *interactive ozone and aerosol in the radiation code*

- *coupled ocean (NEMO) in ORCA025_Z75 configuration*

- *dynamically calculated dry deposition velocities for aerosol*

- *new sea-salt emission scheme based on Grythe et al. (2014)*

- *emissions from volcanic outgassing accounting for sub-grid-scale height of source*

- GFASv1.2 fire emissions

- IFS model resolution T511L60

- analysis resolution T159/T95, using 12h 4D-Var and VarBC

- analysis windows from 15-3UTC and 3-15UTC

- time period 20170501 -

- Blacklist: default CAMS cy45r1 blacklist

- code branch: cxzk_CY45R1_COMPO_fixes

- scripts branch: cxzk_CY45R1_COMPO_fixes

This description (change log) of the e-suite system is given at
https://atmosphere.copernicus.eu/change-log-e-suite-cy45r1-gu42.

2. Upgrade evaluation results: e-suite versus o-suite

2.1 Aerosol evaluation

2.1.1 Total AOD

The evaluation wrt to global aerosol optical properties is done for June to November 2017, (experiment ECMWF_GU42). These months were available fully at the time of evaluation. AeroCom tools have been applied and image catalogues are available at http://aerocom.met.no/cgi-bin/aerocom/surfobs_annualrs.pl?PROJECT=CAMS&MODELLIST=CAMS-e-suite.

Only the SON 2017 figures are shown in Figure 2.1.1 to reflect the latest version of the model. Sea salt AOD in the e-suite was very different during summer and less so in autumn compared to the o-suite. The general increase is probably due to a new sea salt source and a bug fix corrected sea salt results after July 2017. Table 2.1.1 shows an almost 3fold increase in sea salt AOD in JJA summer from o-suite to e-suite and a 50% increase in autumn. This is somehow balanced by a decrease in sulfate and organic AOD in summer. In autumn other AOD components do not change so much compared to the o-suite, leading to an overall increase in total AOD of +13%, e-suite versus o-suite. The maps in figures 2.1.1 indicate that there is more sea salt in remote stormy regions. Figure 2.1.2 reveals more organic AOD, particularly in remote areas and in the Southern high latitudes. Sea salt and organic AOD is increased by 65% and 11% in autumn in the e-suite, while black carbon AOD is overall decreased a little. Figure 2.1.3 shows that all bias indicators (MNMB, FGE, NMB) go up. The AOD as shown in Figure 2.1.4 indicates also some bias increase spatially in coastal/ocean regions. The size of the aerosol is almost as well represented as in the o-suite, but the RMS increases and correlation is reduced from 0.75 to 0.71, see Fig 2.1.5.

Table 2.1.1: Mean global total and speciated AOD in e-suite and o-suite for summer (June, July and August) 2017 and autumn (September, October and November) 2017. More total AOD in e-suite is mainly due to overall more sea salt. Noteworthy is the largest contribution from sea salt to total AOD and the change of organic AOD in e-suite compared to o-suite in summer 2017 and autumn 2017.

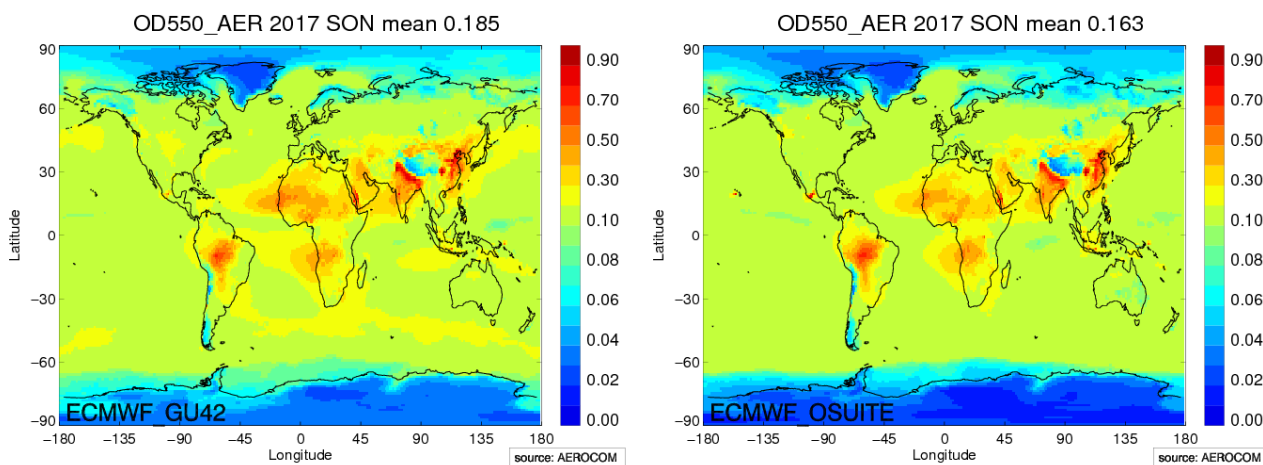|	JJA2017		SON2017	
	e-suite	o-suite	e-suite	o-suite
OD550_aer	0.187	0.166	0.185	0.163
OD550_BC	0.005	0.011	0.007	0.009
OD550_DUST	0.027	0.026	0.016	0.017
OD550_OA	0.055	0.059	0.068	0.061
OD550_SO4	0.033	0.046	0.038	0.040
OD550_SS	0.066	0.024	0.055	0.036

Fig. 2.1.1. Averaged aerosol optical depth (AOD) from e-suite (left) and o-suite (right) IFS model for September-November 2017. Mean AOD in e-suite is at 0.185, which is 13% more than what was in the o-suite. E-suite increase is seen in particular in remote regions.
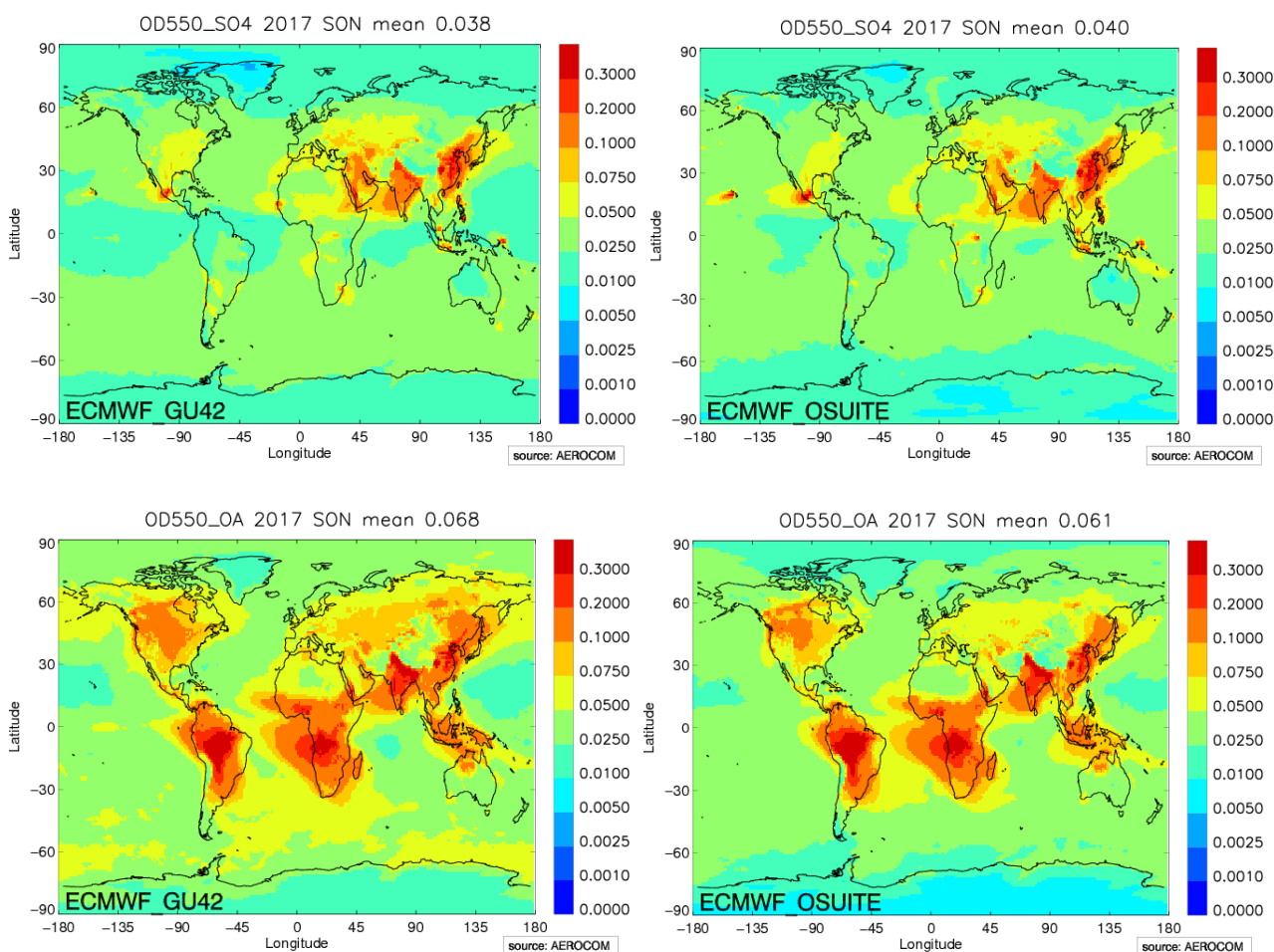

Fig. 2.1.2. Averaged sulfate optical depth in upper row (e-suite (left) and o-suite (right)) and organic aerosol optical depth lower row, for September-November 2017. Globally, mean sulphate AOD is almost equal in the two suites, but for the e-suite sulphate AOD is higher in remote areas and in the Southern Hemisphere. Also the e-suite organic AOD reaches more remote areas.
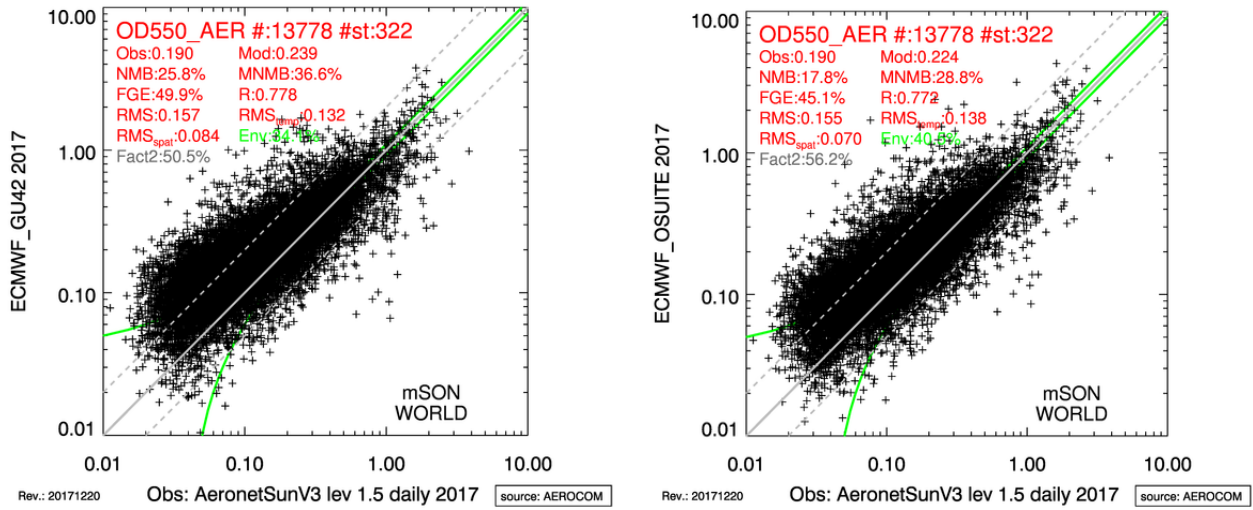
Fig. 2.1.3. Evaluation of simulated daily AOD against Aeronet NRT version 3, level 1.5 photometer measurements in e-suite (left) and o-suite (right) for the period September-November 2017. The new sea salt source (and more organic aerosol) creates an increase in AOD, globally +10%. This makes FGE, MNMB, NMB against Aeronet increase.
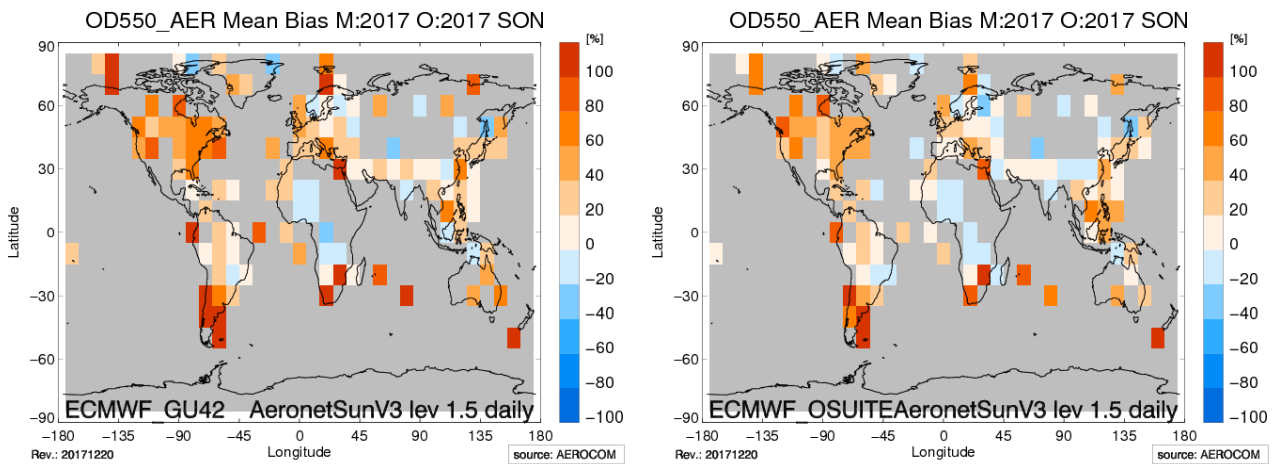

Fig. 2.1.4. Regional relative mean bias of simulated daily AOD against NRT level 1.5 Aeronet SunV3 photometer measurements in e-suite (left) and o-suite (right) for the period September-November 2017. Coastal and sea areas exhibit an AOD bias higher in the e-suite than o-suite, because of the new sea salt source and more organic aerosol.
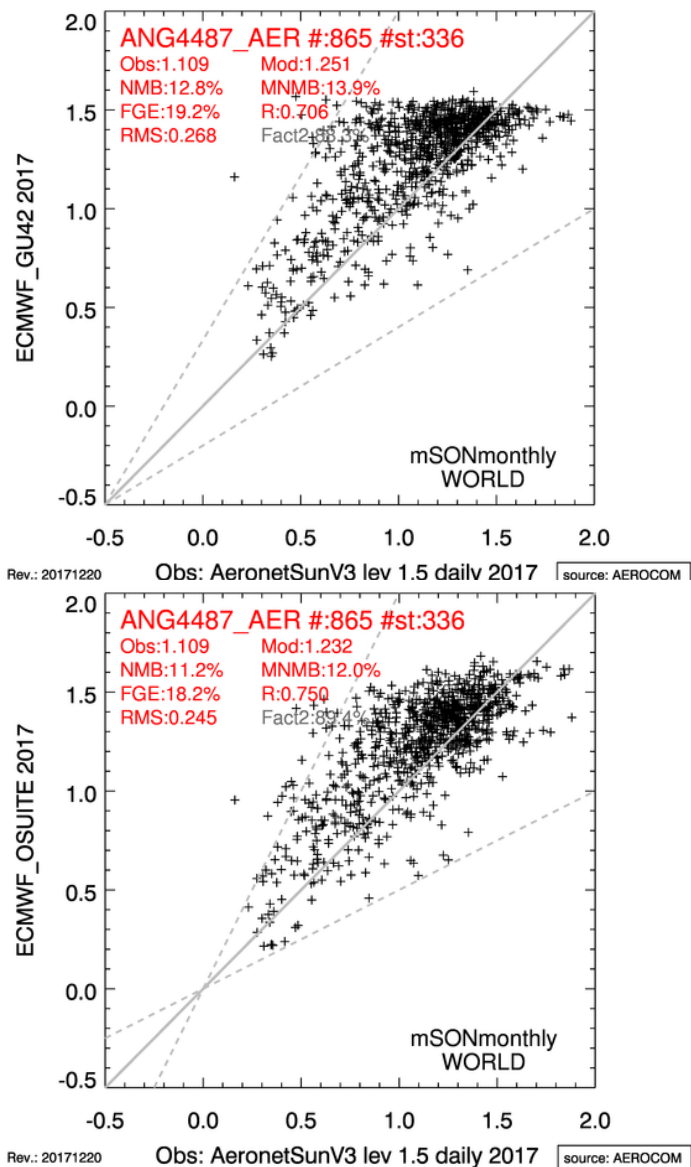
Fig 2.1.5. Angström Exponent scatterplots (e-suite left, o-suite right). The bias has not changed much, but indicators reflect more fine particles and less correlation.

2.1.2 Dust

	NDATA	e-suite MB	FGE	RMSE	r	o-suite MB	FGE	RMSE	r	SDS-WAS MB	FGE	RMSE	r
Sahara	48	-0.32	-0.46	0.49	0.17	-0.38	-0.58	0.54	0.06	-0.42	-0.64	0.55	0.15
Sahel	727	-0.19	-0.44	0.30	0.70	-0.21	-0.43	0.32	0.70	-0.21	-0.42	0.32	0.72
Tropical North Atlantic	13	-0.17	-0.45	0.20	0.85	-0.19	-0.50	0.23	0.86	-0.22	-0.62	0.25	0.90
Subtropical North Atlantic	603	-0.04	-0.06	0.17	0.83	-0.06	-0.14	0.18	0.82	-0.10	-0.34	0.21	0.83
North Western Maghreb	76	-0.12	-0.65	0.17	0.88	-0.14	-0.70	0.18	0.87	-0.14	-0.63	0.18	0.88
Western Iberian Peninsula	654	-0.04	0.36	0.08	0.74	-0.05	0.33	0.09	0.76	-0.05	0.27	0.09	0.75
Iberian Peninsula	1136	-0.02	1.09	0.07	0.82	-0.02	1.07	0.07	0.80	-0.02	1.05	0.08	0.82
Western Mediterranean	2959	-0.03	0.90	0.09	0.84	-0.03	0.88	0.09	0.82	-0.03	0.90	0.09	0.82
Central Mediterranean	2853	-0.01	1.12	0.07	0.88	-0.02	1.10	0.07	0.88	-0.02	1.09	0.08	0.87
Eastern Mediterranean	1924	0.00	1.62	0.07	0.91	0.00	1.61	0.08	0.91	-0.01	1.60	0.09	0.88
Eastern Sahara	111	0.07	0.97	0.09	0.86	0.03	0.81	0.07	0.87	0.02	0.80	0.08	0.82
Middle East	1070	-0.13	-0.24	0.21	0.80	-0.15	-0.32	0.23	0.81	-0.14	-0.20	0.24	0.72
All sites	12174	-0.04	0.81	0.13	0.87	-0.05	0.78	0.14	0.87	-0.05	0.78	0.14	0.87

Table 2.1.2. Dust skill scores (MB, FGE, RMSE and r) of 24h forecasts for CAMS e-suite, CAMS o-suite and SDS-WAS Multi-model Median for JJA 2017, and the number of data (NDATA) used. Dust AOD (DOD) from AERONET is the reference. Both CAMS experiments show similar results which are comparable with the SDS-WAS Multi-model.

	NDATA	e-suite MB	FGE	RMSE	r	o-suite MB	FGE	RMSE	r	SDS-WAS MB	FGE	RMSE	r
Sahara	253	-0.02	0.06	0.11	0.86	-0.03	0.01	0.11	0.88	-0.04	-0.12	0.10	0.91
Sahel	1215	-0.20	-0.50	0.30	0.63	-0.21	-0.51	0.30	0.66	-0.16	-0.32	0.27	0.67
Tropical North Atlantic	50	-0.06	-0.37	0.13	0.72	-0.07	-0.38	0.14	0.72	-0.08	-0.45	0.14	0.75
Subtropical North Atlantic	353	-0.03	-0.21	0.11	0.72	-0.04	-0.20	0.11	0.72	-0.05	-0.27	0.11	0.64
North Western Maghreb	105	-0.10	-0.84	0.19	0.74	-0.11	-0.84	0.19	0.78	-0.12	-0.83	0.21	0.71
Western Iberian Peninsula	513	-0.02	0.81	0.05	0.74	-0.02	0.82	0.05	0.74	-0.03	0.71	0.05	0.77
Iberian Peninsula	793	-0.01	1.28	0.04	0.79	-0.01	1.29	0.04	0.78	-0.02	1.18	0.04	0.79
Western Mediterranean	1692	-0.01	1.36	0.05	0.67	-0.01	1.36	0.05	0.67	-0.01	1.33	0.05	0.72
Central Mediterranean	1423	-0.02	1.01	0.07	0.79	-0.02	0.99	0.07	0.78	-0.02	1.21	0.07	0.74
Eastern Mediterranean	893	-0.02	1.13	0.08	0.75	-0.02	1.14	0.08	0.73	-0.03	1.12	0.08	0.82
Eastern Sahara	188	0.01	0.52	0.06	0.82	0.00	0.46	0.05	0.85	0.00	0.51	0.05	0.87
Middle East	353	-0.09	-0.03	0.17	0.75	-0.12	-0.09	0.27	0.59	-0.12	-0.15	0.27	0.60
All sites	7831	-0.05	0.70	0.14	0.84	-0.05	0.69	0.15	0.84	-0.05	0.70	0.14	0.85

Table 2.1.3. Dust skill scores (MB, FGE, RMSE and r) of 24h forecasts for CAMS e-suite, CAMS o-suite and SDS-WAS Multi-model Median for SON 2017, and the number of data (NDATA) used. Dust AOD (DOD) from AERONET is the reference. Both CAMS experiments show similar results which are comparable with the SDS-WAS Multi-model.

	NDATA	e-suite				o-suite			
		MB	FGE	RMSE	r	MB	FGE	RMSE	r
Sahara	48	-0.22	-0.26	0.44	0.10	-0.22	-0.26	0.45	0.00
Sahel	785	0.03	0.13	0.25	0.61	-0.02	0.05	0.23	0.68
Tropical North Atlantic	13	0.05	0.15	0.12	0.84	0.02	0.09	0.10	0.88
Subtropical North Atlantic	768	0.09	0.82	0.17	0.85	0.08	0.77	0.17	0.83
North Western Maghreb	77	0.05	0.10	0.13	0.88	-0.01	-0.08	0.12	0.87
Western Iberian Peninsula	1128	0.03	0.23	0.09	0.71	0.04	0.23	0.14	0.51
Iberian Peninsula	1729	0.03	0.24	0.07	0.77	0.02	0.19	0.08	0.71
Western Mediterranean	4164	0.04	0.26	0.11	0.74	0.03	0.19	0.11	0.70
Central Mediterranean	3810	0.06	0.32	0.11	0.77	0.05	0.24	0.10	0.78
Eastern Mediterranean	2534	0.03	0.17	0.09	0.75	0.00	0.07	0.10	0.69
Eastern Sahara	220	0.21	0.94	0.22	0.48	0.18	0.87	0.19	0.47
Middle East	1563	0.07	0.21	0.14	0.87	0.01	0.10	0.13	0.86
All sites	16839	0.05	0.28	0.12	0.81	0.03	0.21	0.12	0.79

Table 2.1.4. Aerosol optical depth skill scores (MB, FGE, RMSE and r) of 24h forecasts for CAMS e-suite and CAMS o-suite for JJA 2017, and the number of data (NDATA) used. AOD from AERONET is the reference. In general, e-suite presents higher overestimation with MB values (0.05) than o-suite (0.03) in average for all the AERONET sites. e-suite shows better results in the Mediterranean than o-suite in terms of correlation. Otherwise, e-suite presents lower correlation values in the Sahel and Tropical N. Atl.

	NDATA	e-suite				o-suite			
		MB	FGE	RMSE	r	MB	FGE	RMSE	r
Sahara	255	0.06	0.45	0.13	0.85	0.04	0.37	0.11	0.88
Sahel	1313	0.03	0.13	0.24	0.54	-0.01	0.04	0.22	0.62
Tropical North Atlantic	50	0.09	0.42	0.13	0.84	0.03	0.21	0.10	0.84
Subtropical North Atlantic	471	0.11	0.84	0.15	0.73	0.09	0.76	0.13	0.72
North Western Maghreb	183	0.06	0.37	0.14	0.71	0.03	0.26	0.13	0.74
Western Iberian Peninsula	820	0.04	0.40	0.08	0.79	0.04	0.36	0.08	0.70
Iberian Peninsula	1303	0.04	0.43	0.07	0.78	0.03	0.33	0.06	0.77
Western Mediterranean	2748	0.04	0.40	0.08	0.77	0.03	0.32	0.07	0.76
Central Mediterranean	2036	0.06	0.42	0.11	0.63	0.04	0.28	0.10	0.63
Eastern Mediterranean	1567	0.05	0.30	0.11	0.70	0.03	0.20	0.11	0.66
Eastern Sahara	313	0.13	0.77	0.15	0.61	0.10	0.67	0.12	0.70
Middle East	929	0.06	0.21	0.10	0.86	0.02	0.10	0.15	0.69
All sites	11988	0.05	0.38	0.12	0.79	0.03	0.28	0.12	0.79

Table 2.1.5. Aerosol optical depth skill scores (MB, FGE, RMSE and r) of 24h forecasts for CAMS e-suite and CAMS o-suite for JJA 2017, and the number of data (NDATA) used. AOD from AERONET is the reference. During autumn, e-suite presents higher overestimation with MB values (0.05) than o-suite (0.03) in average for all the AERONET sites. e-suite shows better results in the Mediterranean and the Middle East than o-suite in terms of correlation. Otherwise, e-suite presents lower correlation values in the Sahel and Tropical N. Atl.
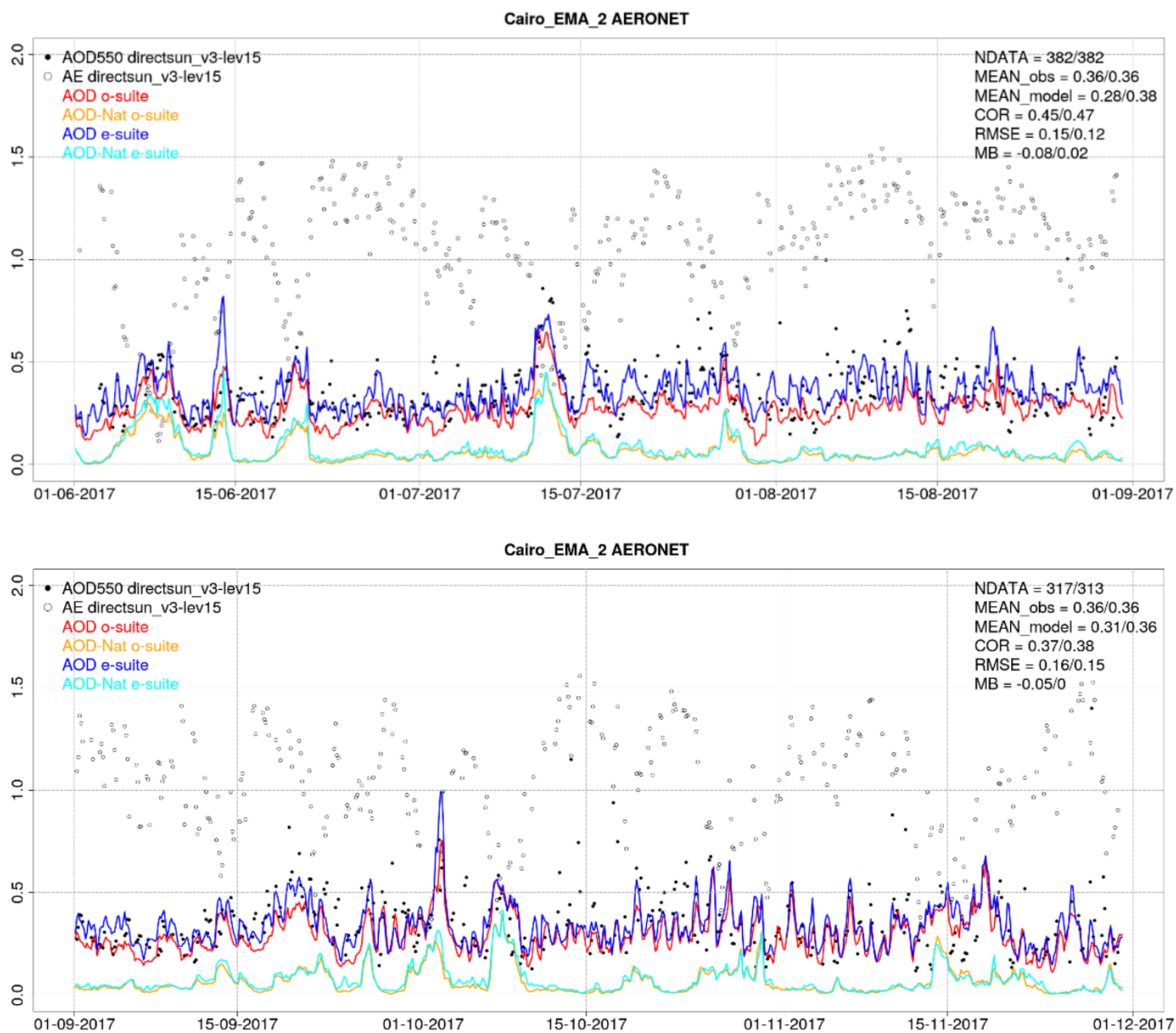
Figure 2.1.6. AOD from AERONET (black dot), AOD o-suite (red line), AOD control (blue line), AOD-Nat o-suite (orange line), AOD-Nat control (cyan line), for the study period over Cairo (Egypt, E. Mediterranean). AOD-Nat corresponds to the natural aerosol optical depth that includes dust and sea-salt. Skill scores per each individual site and model (o-suite/e-suite) are shown in the upper right corner (NDATA: available 3-hourly values used for the calculations, MEAN observations, MEAN_model, COR, RMSE, MB). In the Mediterranean, e-suite presents higher background levels than o-suite. MB increases from -0.08 (-0.05) for o-suite to 0.02 (0) for e-suite in Cairo_EMA in summer (autumns) that are not associated to natural aerosols.

VENACO(FRANCIA; RUR) AIRBASE

NDATA = 412/412 || NDATA = 239/256
MEAN_obs = 10.47/10.47 || MEAN_obs = 7.19/7.33
MEAN_model = 26.27/17.35 || MEAN_model = 9.65/13.32
COR = -0.01/0.37 || COR = 0.46/0.32
RMSE = 122.47/12.49 || RMSE = 6.16/10.83
MB = 15.8/6.88 || MB = 2.47/5.99

VENACO(FRANCIA; RUR) AIRBASE

NDATA = 639/631 || NDATA = 133/133
MEAN_obs = 8.02/8 || MEAN_obs = 6.83/6.83
MEAN_model = 12.14/12.32 || MEAN_model = 7/6.59
COR = 0.43/0.3 || COR = 0.05/0.07
RMSE = 16.95/15.06 || RMSE = 14.41/14.76
MB = 4.12/4.32 || MB = 0.16/-0.25

Figure 2.1.7. PM10 and PM2.5 EIONET-Airbase observations (black and grey dots, respectively), PM10 and PM2.5 o-suite (red and orange lines, respectively) and PM10 and PM2.5 e-suite (blue and cyan lines, respectively) for the study period (JJA and SON) over Venaco (Corse, France). Skill scores per each individual site, model (o-suite/e-suite) and PM10/PM2.5 are shown in the upper right corner (NDATA: available 3-hourly values used for the calculations, MEAN observations, MEAN_model, COR, RMSE, MB). At surface levels, the maximum PM10 and PM2.5 levels simulated by e-suite present differences with respect o-suite in maritime sites as Venaco. These maximum PM10 and PM2.5 peaks are linked to sea-salt contribution. This is because the e-suite includes changes in the sea-salt component (a new sea-salt emission).

2.2 Verification of tropospheric ozone

2.2.1 Verification with sonde data in the free troposphere
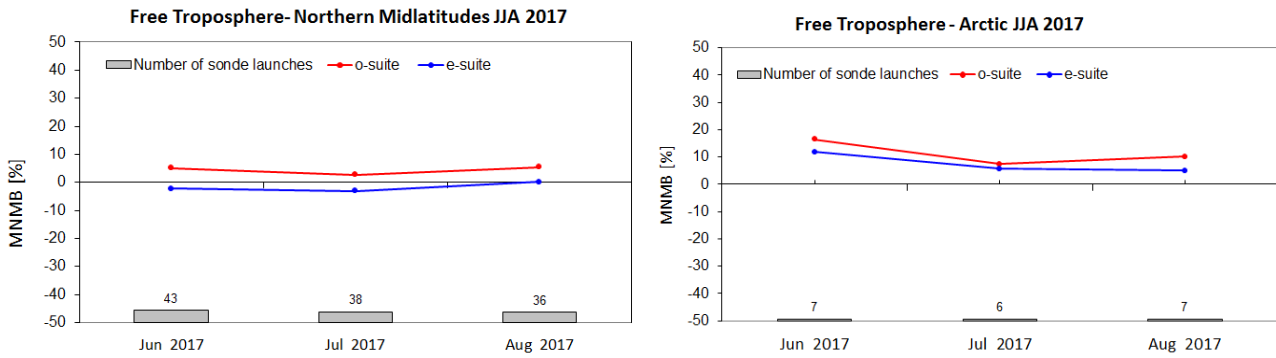
Fig. 2.2.1: MNMBs (%) of ozone in the free troposphere (between 750 and 200 hPa (Tropics) / 300 hPa) from the IFS model runs against aggregated sonde data over the Northern Midlatitudes (left) and Arctic (right). The numbers indicate the amount of individual number of sondes.
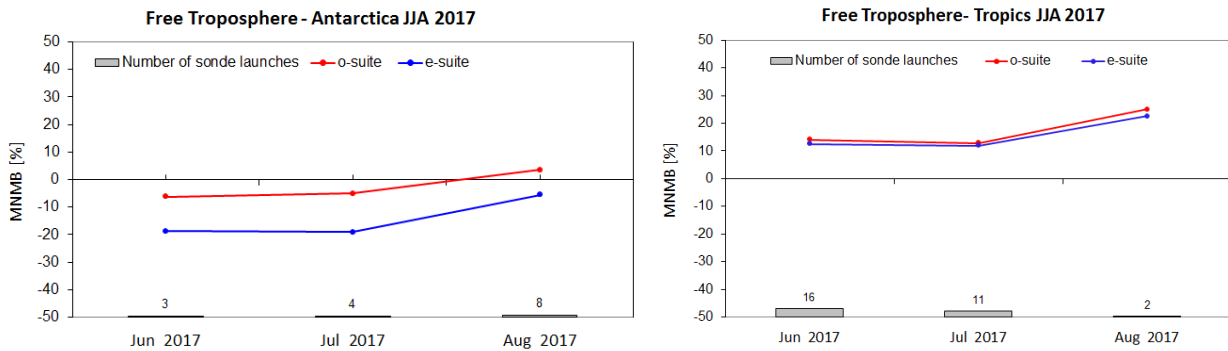
Fig. 2.2.2: MNMBs (%) of ozone in the free troposphere (between 750 and 200 hPa (Tropics) / 300 hPa) from the IFS model runs against aggregated sonde data over the Tropics (left) and Antarctica (right). The numbers indicate the amount of individual number of sondes.

2.2.2 Verification with GAW and ESRL-GMD surface observations
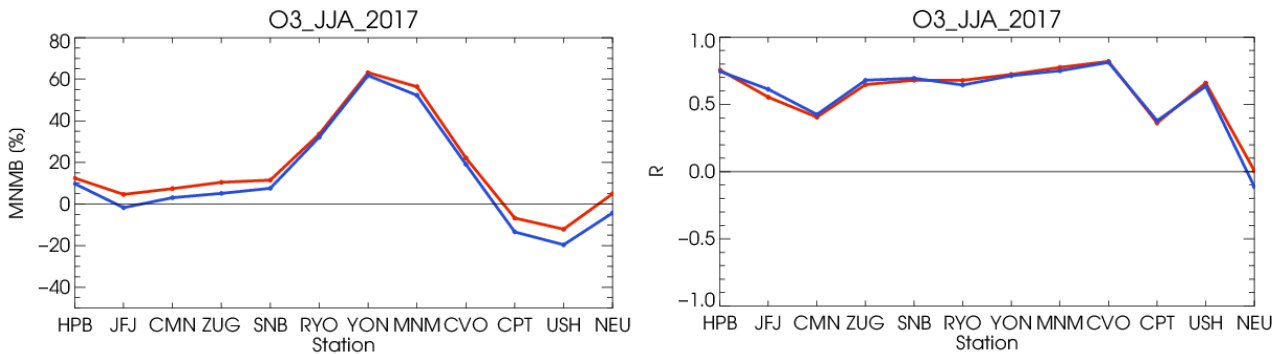
Fig. 2.2.3: MNMB [%] (left) and R (right) for the evaluation of modelled O3 surface mixing ratios with observations of 12 GAW stations. Bottom: MNMB for June-August 2017. The difference between o-suite and e-suite increases towards higher latitudes.
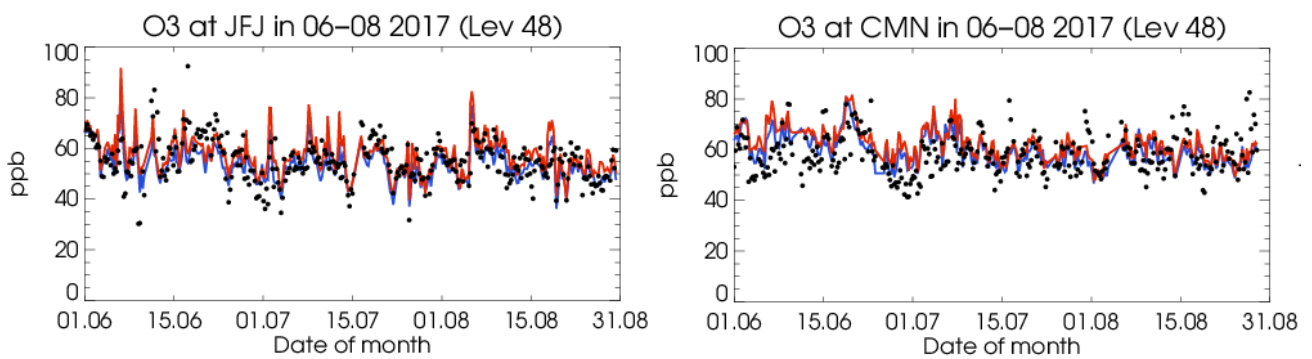
Fig. 2.2.4: Time series of ozone volume mixing ratio (ppbv) for the o-suite (red) and e-quite (blue) compared to GAW observations at Jungfraujoch (left) and Monte Cimone (right).
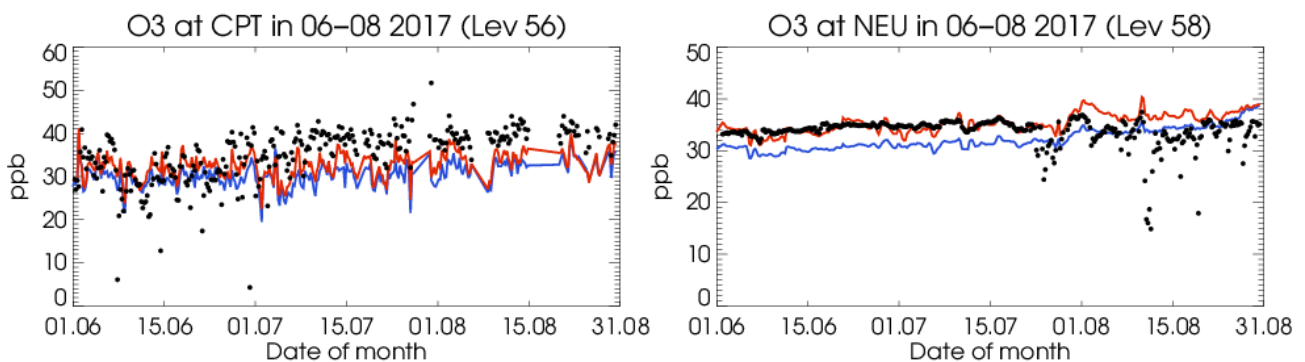
Fig. 2.2.5: Time series of ozone volume mixing ratio (ppbv) for the o-suite (red) and e-quite (blue) compared to GAW observations at Cape Point (left) and Neumayer (right).
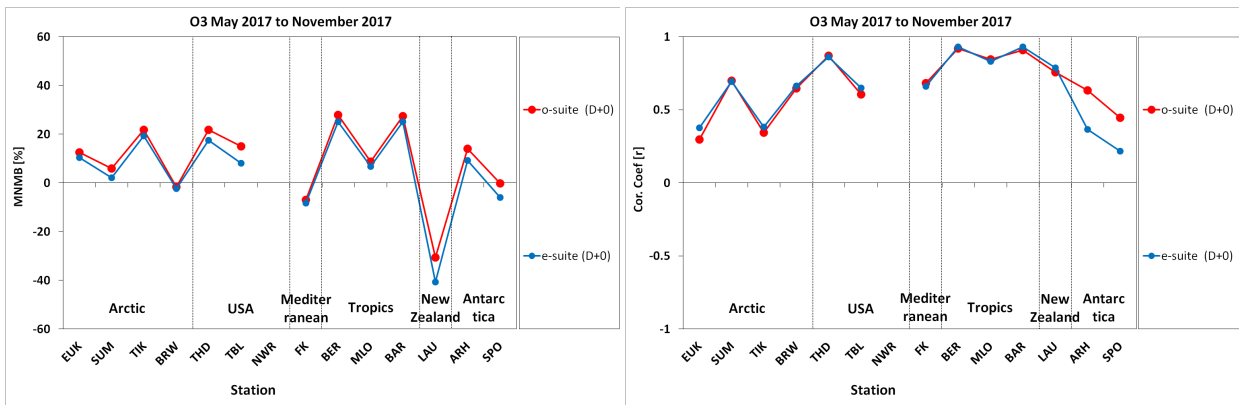
Fig. 2.2.6: MNMB [%] (left) and R (right) for the evaluation of modelled O3 surface mixing ratios with observations of 13 ESRL stations Period: May 2017 - November 2017.
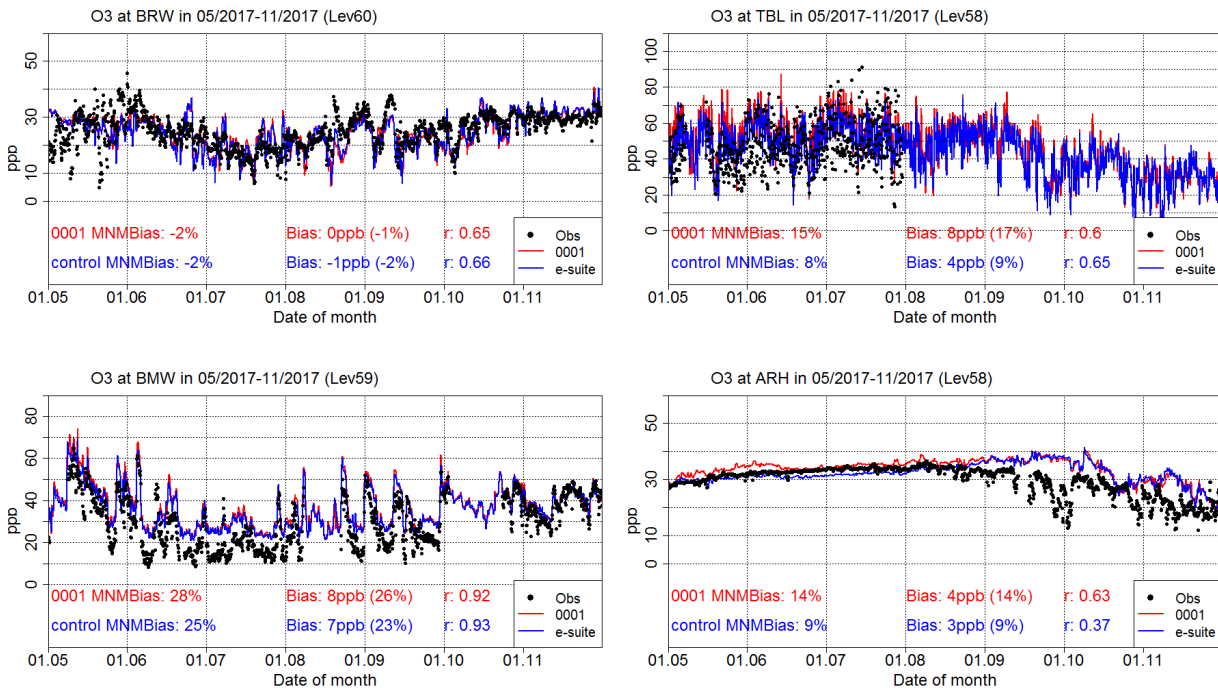
Fig. 2.2.7: Time series of ozone volume mixing ratio (ppbv) for the o-suite (red) and e-suite (blue) compared to ESRL observations at Point Barrow, Alaska USA (71.32°N, 156.61°W, upper left), Table Mauntain, USA (40.12°N, 105.24°W upper right), at Tudor Hill, Bermuda (32.27°N, 64.88°W, lower left right), and Arrival Heights, Antarctica (77.83°S, 166.20°E, lower right)

2.2.3 Verification with IAGOS ozone observations

The e-suite dataset associated to experiment gu42 has been validated against IAGOS data for the 6 months period between June and November 2017. During this period, there have been observations almost every day at Paris.

Fig. 2.2.9 and 2.2.10 show the timeseries of the differences (model analysis- observations) and relative differences ((model analysis – observations)/observations) in the daily profiles for ozone during the period June-August and September-November 2017 respectively. Overestimations by the models are displayed in red colors, and underestimations in blue colors. On these time series, it can be seen that there are no notable differences between e-suite and o-suite results. The differences are more pronounced in the UTLS with mostly overestimations. Relative differences also present large values in the UTLS, and also in the surface and boundary layer especially in the JJA period. In general, the best agreement is found in the free troposphere for both models, where absolute values of these differences and relative differences are smaller.

Although both models often overestimate at the surface and boundary layer in JJA period (Fig. 2.2.8), this might not be the case during episodes of pollution transport. Around 21 June, the transport of pollution from forest fires in Portugal and Spain has been observed by IAGOS as reported in CAMS84 JJA 2017 reports for global and regional. For this episode (Fig. 2.2.8), the results for the e-suite are very similar to those of the o-suite and show large underestimations of ozone from the surface to the free troposphere. On the 28 December (Fig. 2.2.9) which might be associated to another pollution transport episode (not documented so far), the models show the same behaviour as for the episode of June.

Fig. 2.2.10 and 2.2.11 displays the timeseries of different monthly scores of the mode analysis for ozone that have been calculated based on the daily profiles. The scores presented here are: the Mean Bias (MB); the Mean Normalized Bias (NMB), the Root Mean Square Error (RMSE) and Fractional Gross Error (FGE). As shown on these figures, the results from o-suite and e-suite are very similar for all types of scores. Ozone is always overestimated in the UTLS as shown by NMB. In the surface and boundary layer the ozone is overestimated between June to October (see NMB). In November, the agreement between models and observations in the surface and boundary layer appears much better, but it should be noted that there is a gap in IAGOS data of about one week during this month.
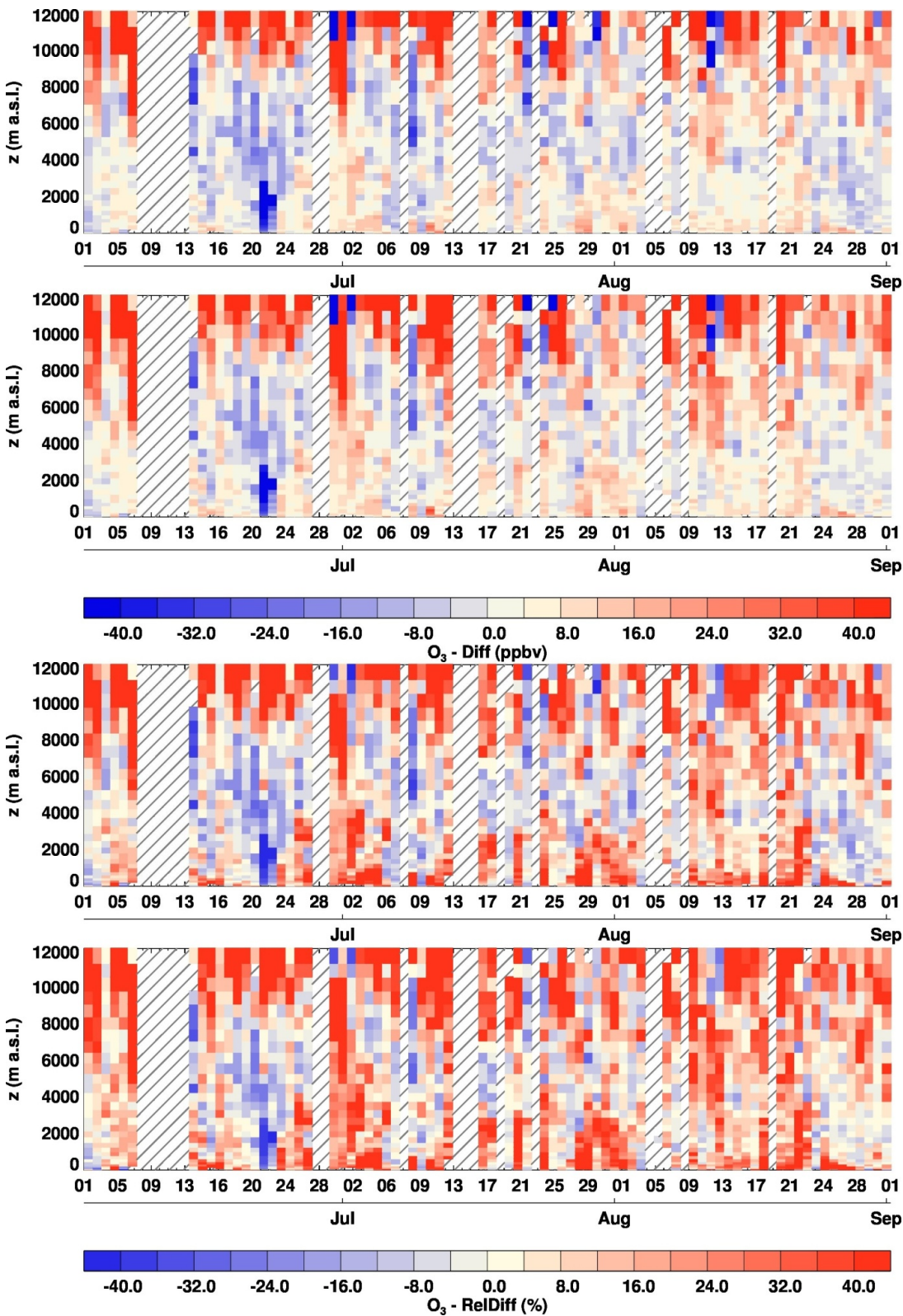
Figure 2.2.8: Time series of ozone differences (ppbv) and relative differences (%) in the mixing ratio profiles (daily) between models (analysis) and observations for the period JJA 2017. From top to bottom: differences for e-suite then for o-suite, and relative differences for e-suite then for o-suite.
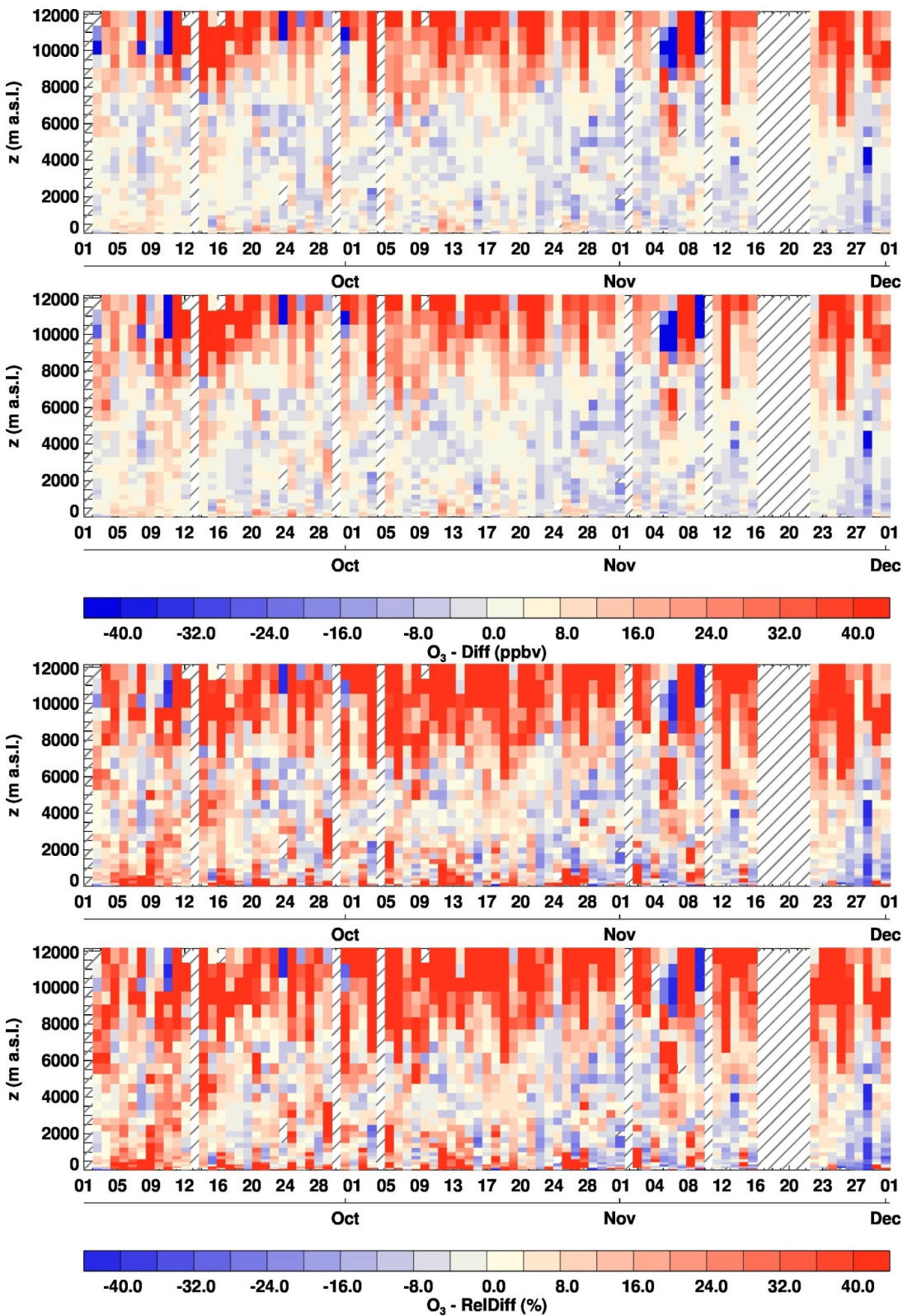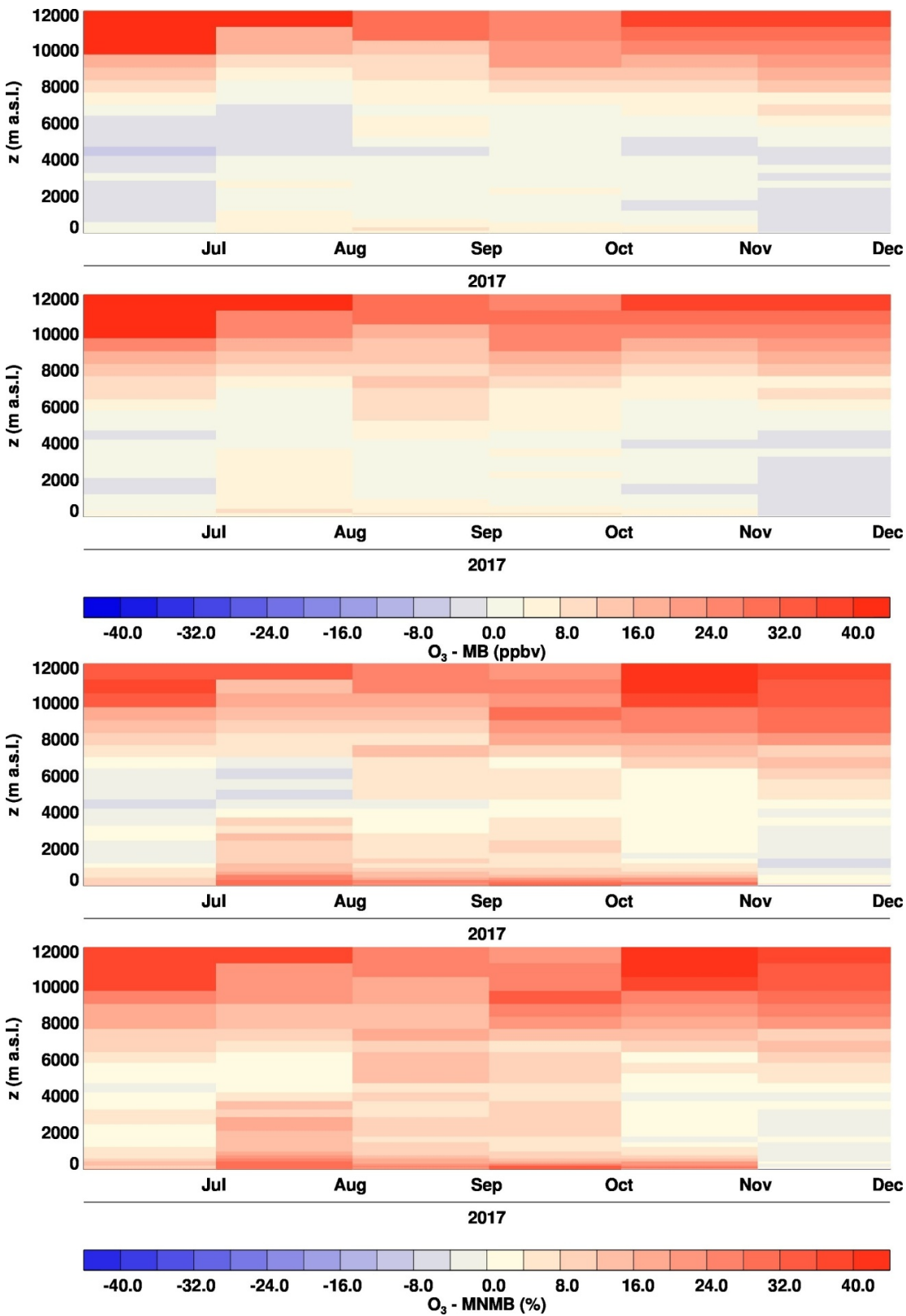
Figure 2.2.9: Time series of ozone differences (ppbv) and relative differences (%) in the mixing ratio profiles (daily) between models (analysis) and observations for the period SON 2017. From top to bottom: differences for e-suite then for o-suite, and relative differences for e-suite then for o-suite.

Figure 2.2.10: Time series of monthly analysis scores (MB in ppbv and NMB in %) for ozone during the period June-November 2017. From top to bottom: Mean Bias (MB) for e-suite then for o-suite, Normalized Mean Bias (NMB) for e-suite then for o-suite.
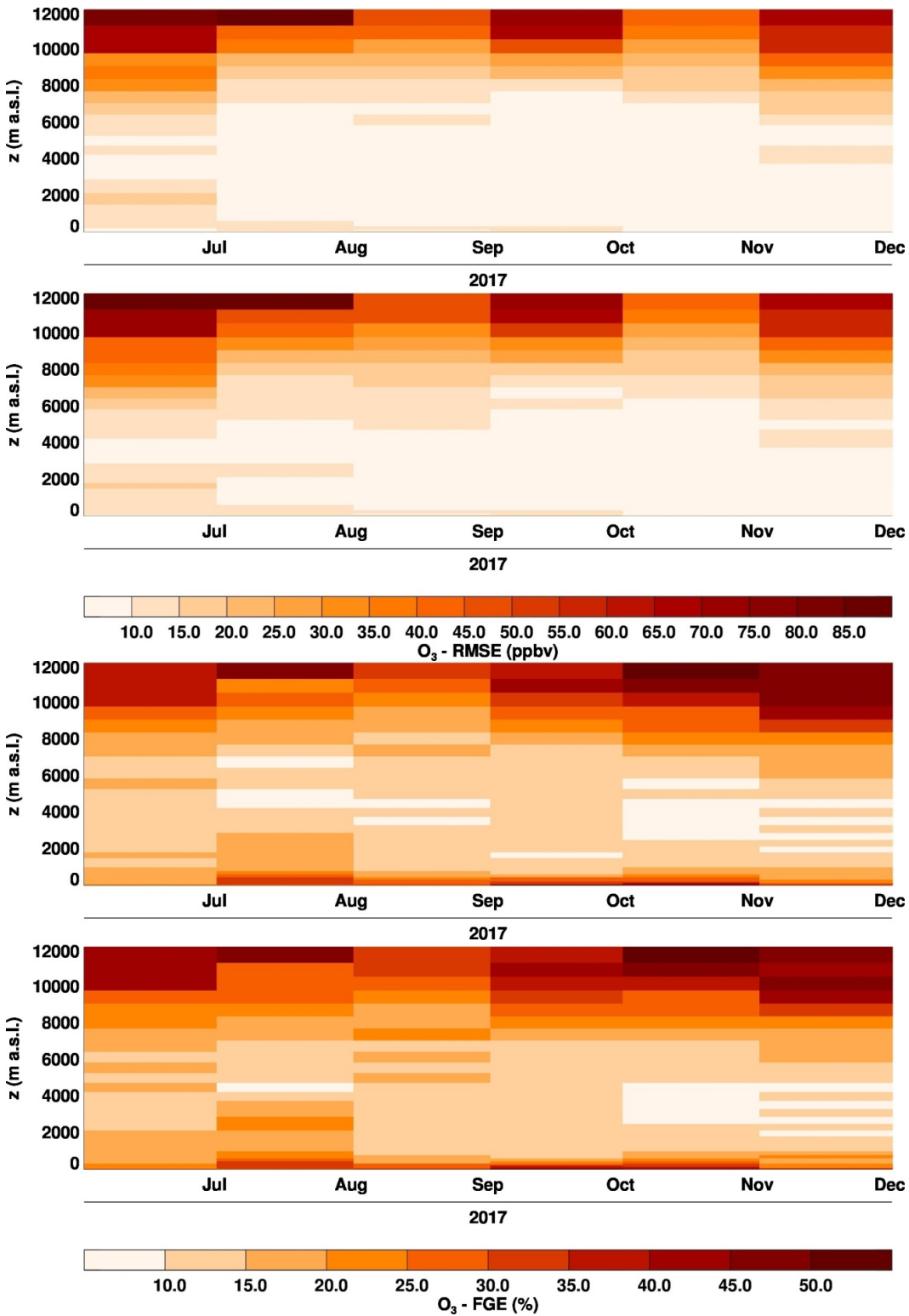
Figure 2.2.11: Time series of monthly analysis scores (RMSE in ppbv, and FGE in %) for ozone during the period June-November 2017. From top to bottom: Root Mean Square Error (RMSE) for e-suite then for o-suite, Fractional Gross Error (FGE) for e-suite then for o-suite.

2.2.4 Verification of ozone in the Mediterranean

Table 2.2.1: Coordinates, elevation, corresponding model level (level 60 is the surface level), as well as validation scores (Biases, MNMBs and correlations for the period 05/2017-11/2017) obtained with the 2 forecast runs (o-suite and e-suite), for each one of the selected Mediterranean stations. Biases, MNMBs and correlations with blue denote stations where e-suite performs better while with red are denoted stations where o-suite performs better. The surface ozone validation analysis over the Mediterranean is based on an evaluation against station observations from the Airbase Network (http://acm.eionet.europa.eu/databases/airbase/). In addition, 2 stations from the Department of Labour Inspection - Ministry of Labour and Social Insurance, of Cyprus (http://www.airquality.dli.mlsi.gov.cy/) are used in the validation analysis. For the validation analysis, stations in the Mediterranean located within about 100 km from the shoreline of the Mediterranean shore are used.

| Station Name	Stat_ID	Lon	Lat	Alt (m)	Level	Distance from the shore (km)	Bias (ppb) o-suite	Bias (ppb) e-suite	MNMB [%] o-suite	MNMB [%] e-suite	Cor. Coef o-suite	Cor. Coef e-suite
Al Cornocales	ES1648A	-5.66	36.23	189	57	16	3.6	2.4	8.0	5.5	0.60	0.58
Caravaka	ES1882A	-1.87	38.12	1	60	73	-14.4	-15.4	-35.8	-38.7	0.69	0.72
Zarra	ES0012R	-1.10	39.08	885	56	70	-8.6	-10.3	-16.7	-19.9	0.83	0.83
VIillar Del Arzobispo	ES1671A	-0.83	39.71	430	60	48	-6.0	-7.3	-16.2	-19.6	0.78	0.81
Cirat	ES1689A	-0.47	40.05	466	60	37	-1.3	-2.2	-3.9	-6.3	0.71	0.74
Bujaraloz	ES1400A	-0.15	41.51	327	60	60	-8.3	-9.2	-29.1	-32.1	0.76	0.76
Morella	ES1441A	-0.09	40.64	1150	53	51	-7.5	-9.2	-14.3	-17.4	0.80	0.80
Bc-La Senia	ES1754A	0.29	40.64	428	59	21	-6.9	-8.1	-17.4	-20.0	0.55	0.57
Ay-Gandesa	ES1379A	0.44	41.06	368	58	15	-1.0	-2.2	-2.3	-4.8	0.80	0.80
Ak-Pardines	ES1310A	2.21	42.31	1226	57	81	3.6	2.7	8.2	6.6	0.65	0.67
Hospital Joan March	ES1827A	2.69	39.68	172	57	3	4.5	3.4	7.6	5.8	0.66	0.66
Al-Agullana	ES1201A	2.84	42.39	214	60	25	-7.0	-7.4	-21.2	-22.2	0.58	0.56
Av-Begur	ES1311A	3.21	41.96	200	56	9	0.5	-0.6	-0.5	-2.4	0.71	0.71
Plan Aups/Ste Baume	FR03027	5.73	43.34	675	54	21	-3.2	-4.8	-6.7	-9.3	0.81	0.80
Gharb	MT00007	14.20	36.07	114	57	31	-7.1	-8.6	-13.1	-15.7	0.63	0.63
Finokalia	GR0002R	25.67	35.32	250	57	4	-3.9	-4.6	-6.9	-8.3	0.68	0.66
Oros Troodos	-	32.86	34.95	1819	49	11	5.8	3.1	11.2	5.9	0.48	0.46
Agia Marina	CY0002R	33.06	35.04	532	55	14	3.4	0.2	5.2	0.8	0.59	0.60
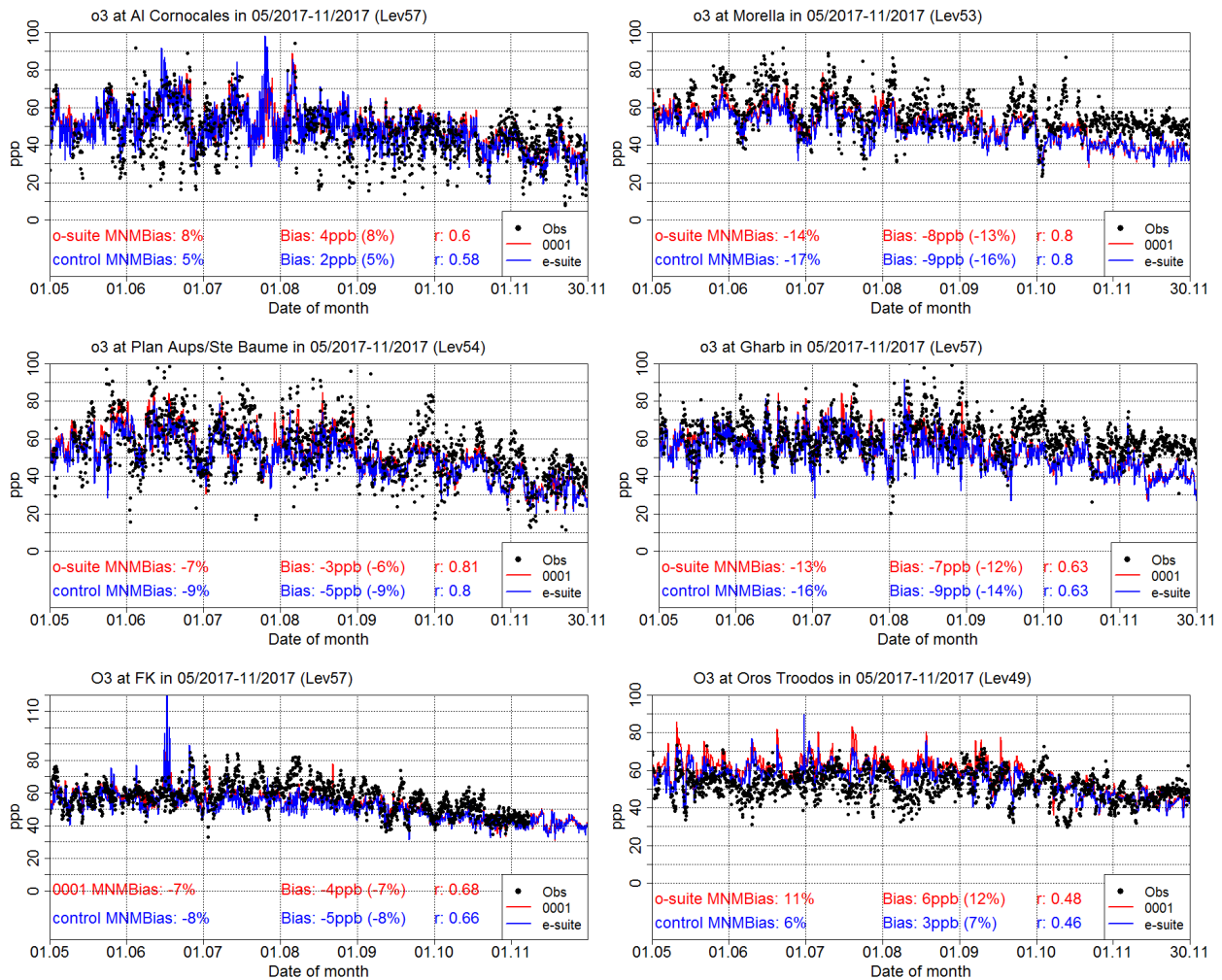
Fig. 2.2.12: Time series of ozone volume mixing ratio (ppbv) for the o-suite (red) and e-suite (blue) compared to AirBase observations at Al Cornocales, Spain(36.23°N, 5.66°W, upper left), Morella, Spain(40.64°N, 0.09°W,upper right), Plan Aups/Ste Baume, France (43.34°N, 5.73°E, middle left), Gharb, Malta (36.07°N, 14.20°E, middle right), Finokalia, Crete station (35.32°N, 25.67°E, lower left) and Mountain Troodos, Cyprus (34.95°N, 32.86°E, lower right).

2.2.5 Verification with ozone surface data in the Arctic
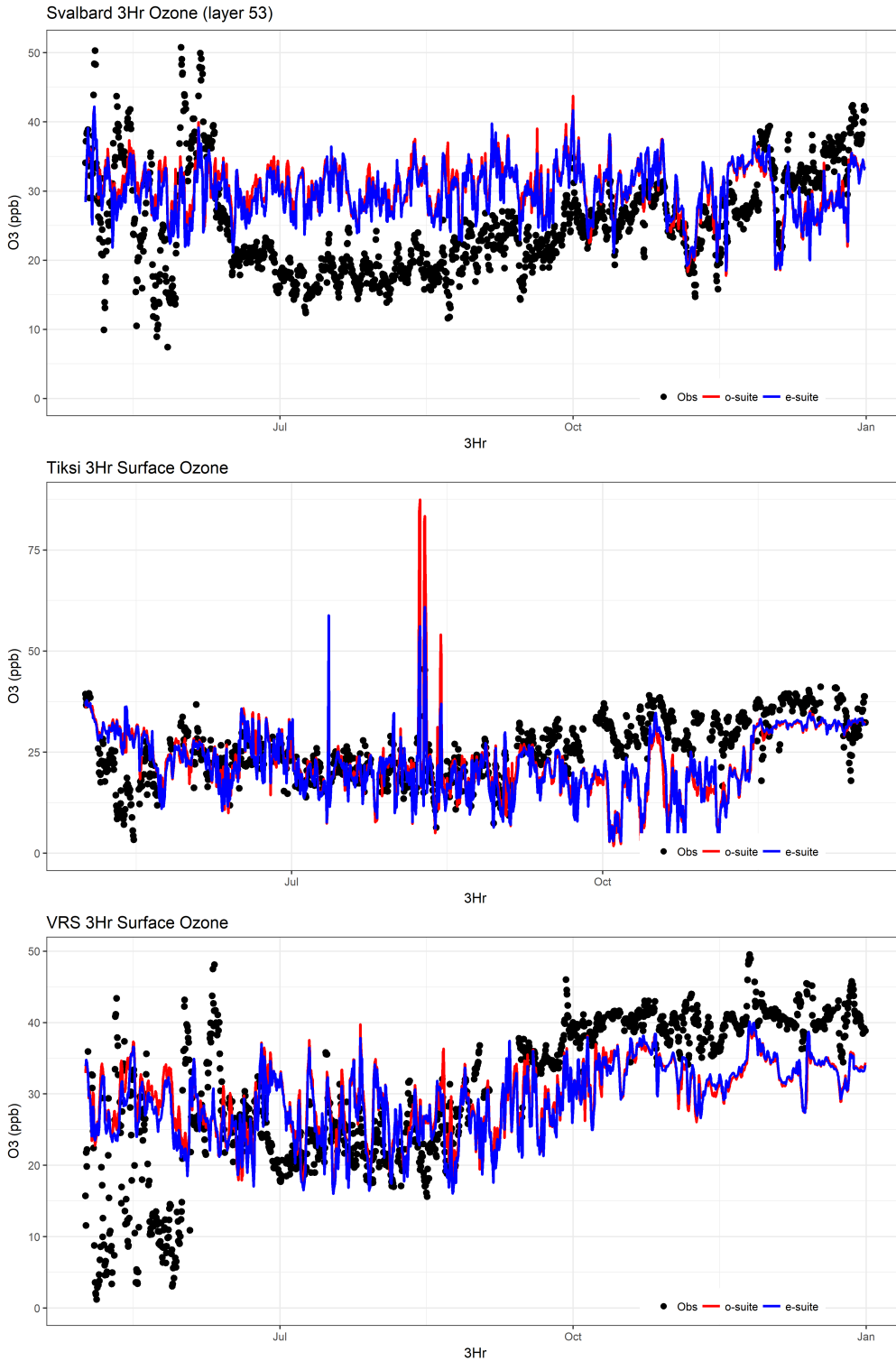
Fig. 2.2.13: Surface ozone concentrations at the Zeppelin Mountain, Svalbard (top left), Tiksi, Russia (top right) and Villum Research Station, Greenland (bottom) from May– December 2017. There are no large differences in the performance of the e-suite and the o-suite for surface ozone at Svalbard, Tiksi and VRS in the Arctic, while the e-suite has higher correlation coefficients for all sites.

2.3 Carbon monoxide

2.3.1 Validation with Global Atmosphere Watch (GAW) Surface Observations
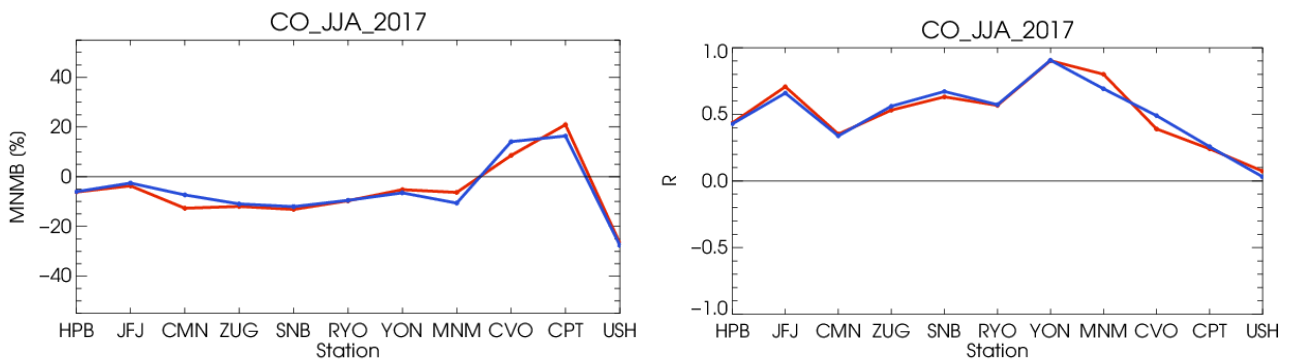
Fig. 2.3.1: MNMB [%] (left) and R (right) for the evaluation of modelled CO surface mixing ratios with observations of 11 GAW stations for the period JJA 2017.
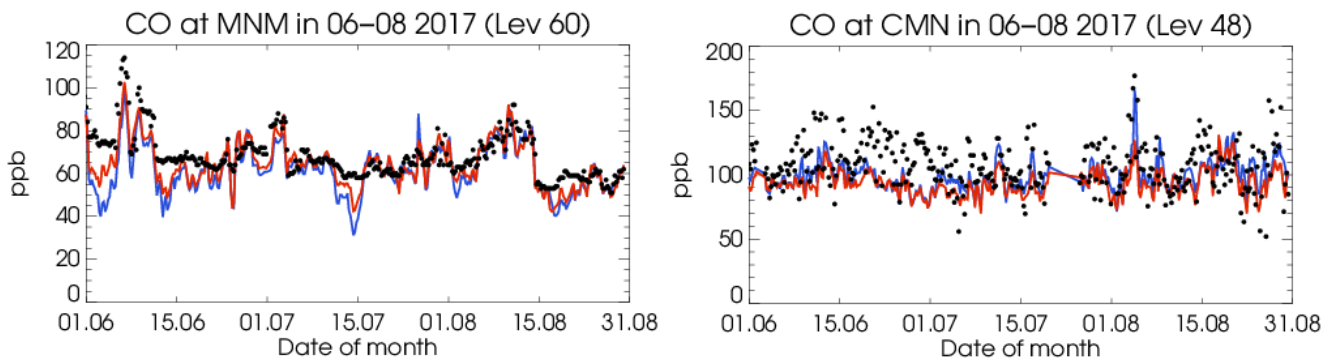
Fig. 2.3.2: Time series of carbon monoxide volume mixing ratio (ppbv) for the o-suite (red) and e-quite (blue) compared to GAW observations at Minamitorishima (left) and Monte Cimone (right).
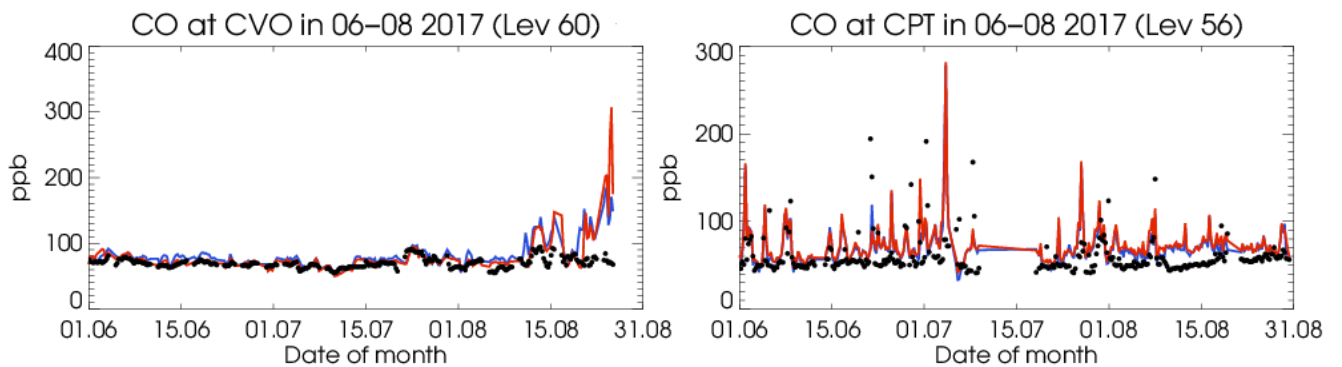
Fig. 2.3.3: Time series of carbon monoxide volume mixing ratio (ppbv) for the o-suite (red) and e-quite (blue) compared to GAW observations at Cape Verde (left) and Cape Point (right).

2.3.2 IAGOS Aircraft observations

The o-suite and e-suite CO concentrations have been compared with IAGOS over Paris during JJA and SON 2017. The timeseries of the differences and relative differences in the daily profile for CO are presented in Fig. 2.3.4 and 2.3.5. during the period June-August and September-November 2017 respectively. Overestimations by the models are displayed in red colors, and underestimations in blue colors. No notable differences between e-suite and o-suite results are found in these timeseries. The same features are obtained for the differences and relative differences in both periods. The daily comparisons show that CO is mostly underestimated in the surface up to the free troposphere, with the largest underestimations often obtained at the surface and boundary layer. In the UTLS CO is often overestimated.

In mid-October Ophelia hurricane have allowed the transport of smoke from severe fires in northern Portugal and Spain to several countries of western Europe, and extreme values of CO have been observed in the boundary layer and free troposphere at Paris (see CAMS validation report for SON 2017). The timeseries of the monthly scores (MB, NMB, RMSE and FGE) for CO from model analysis are presented in Fig. 2.3.6 and 2.3.7. As shown on these figures, the results from o-suite and e-suite are very similar for all types of scores. The episode related to Ophelia can be clearly seen in the representation of the FGE score which present extremely large values at an altitude of about 1500 m as compared to other months
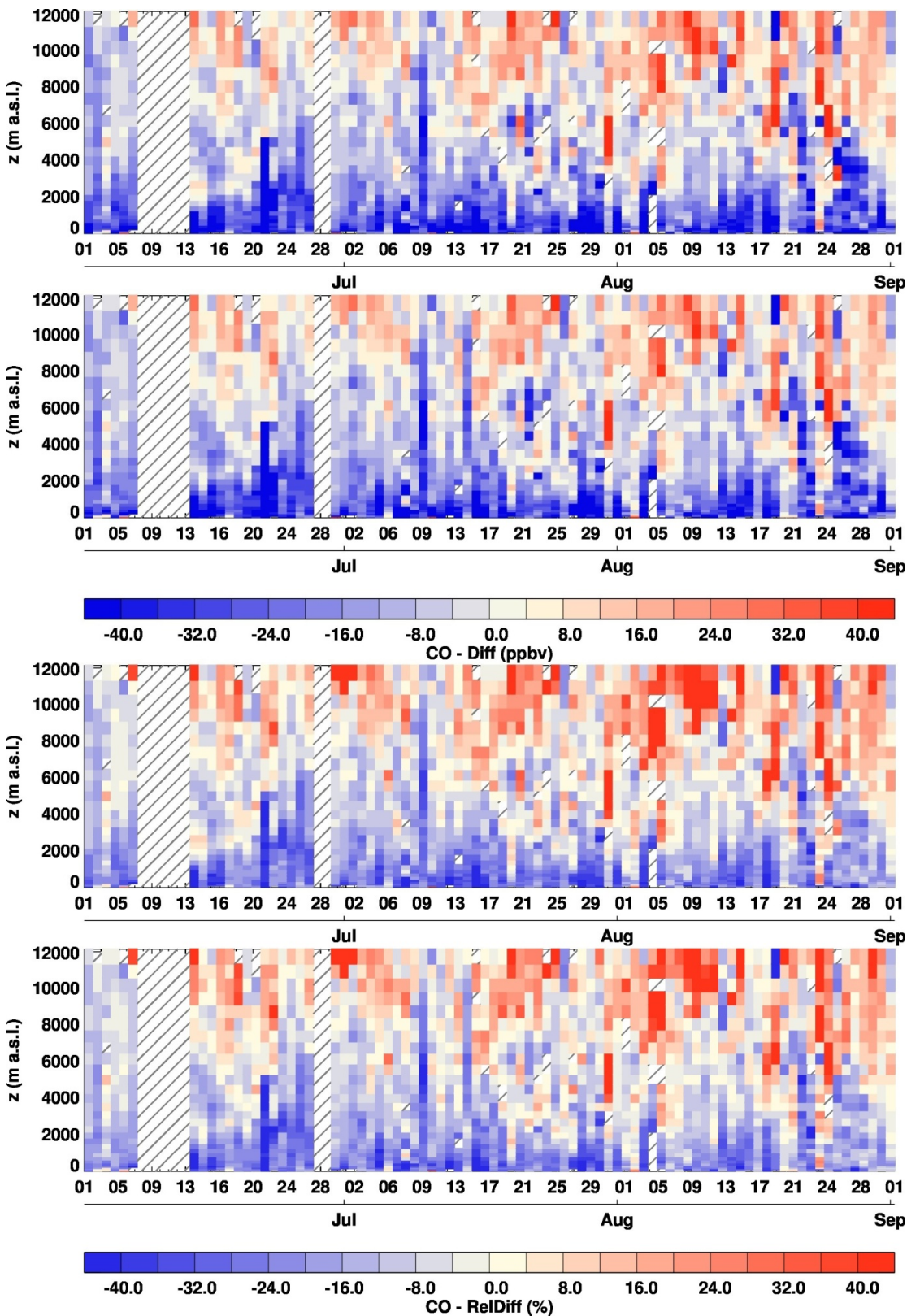
Figure 2.3.4: Time series of CO differences and relative differences in the mixing ratio profiles (daily) between models (analysis) and observations for the period JJA 2017. From top to bottom: differences for e-suite then for o-suite, and relative differences for e-suite then for o-suite.
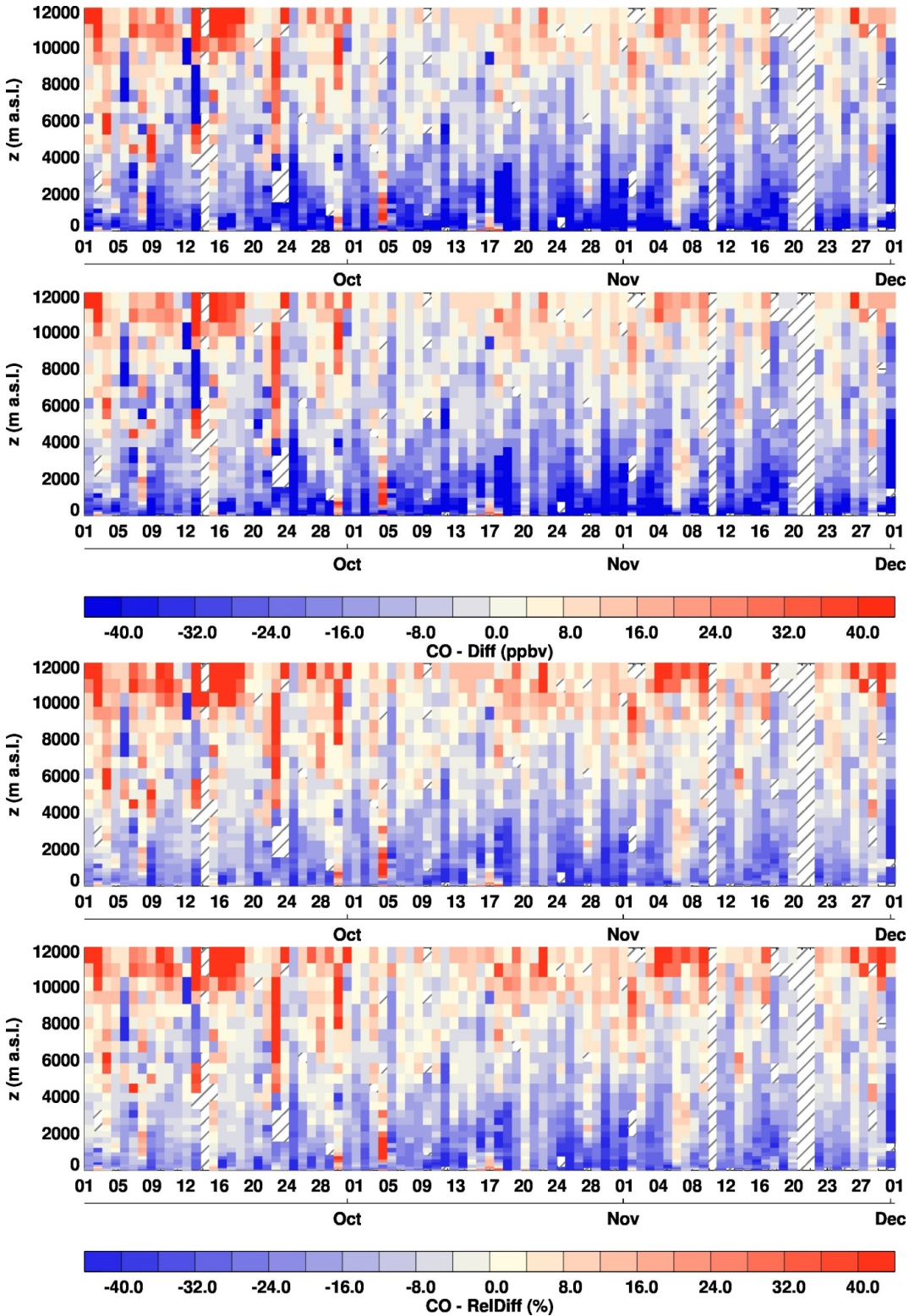
Figure 2.3.5: Time series of CO differences (ppbv) and relative differences (%) in the mixing ratio profiles (daily) between models (analysis) and observations for the period SON 2017. From top to bottom: differences for e-suite then for o-suite, and relative differences for e-suite then for o-suite.
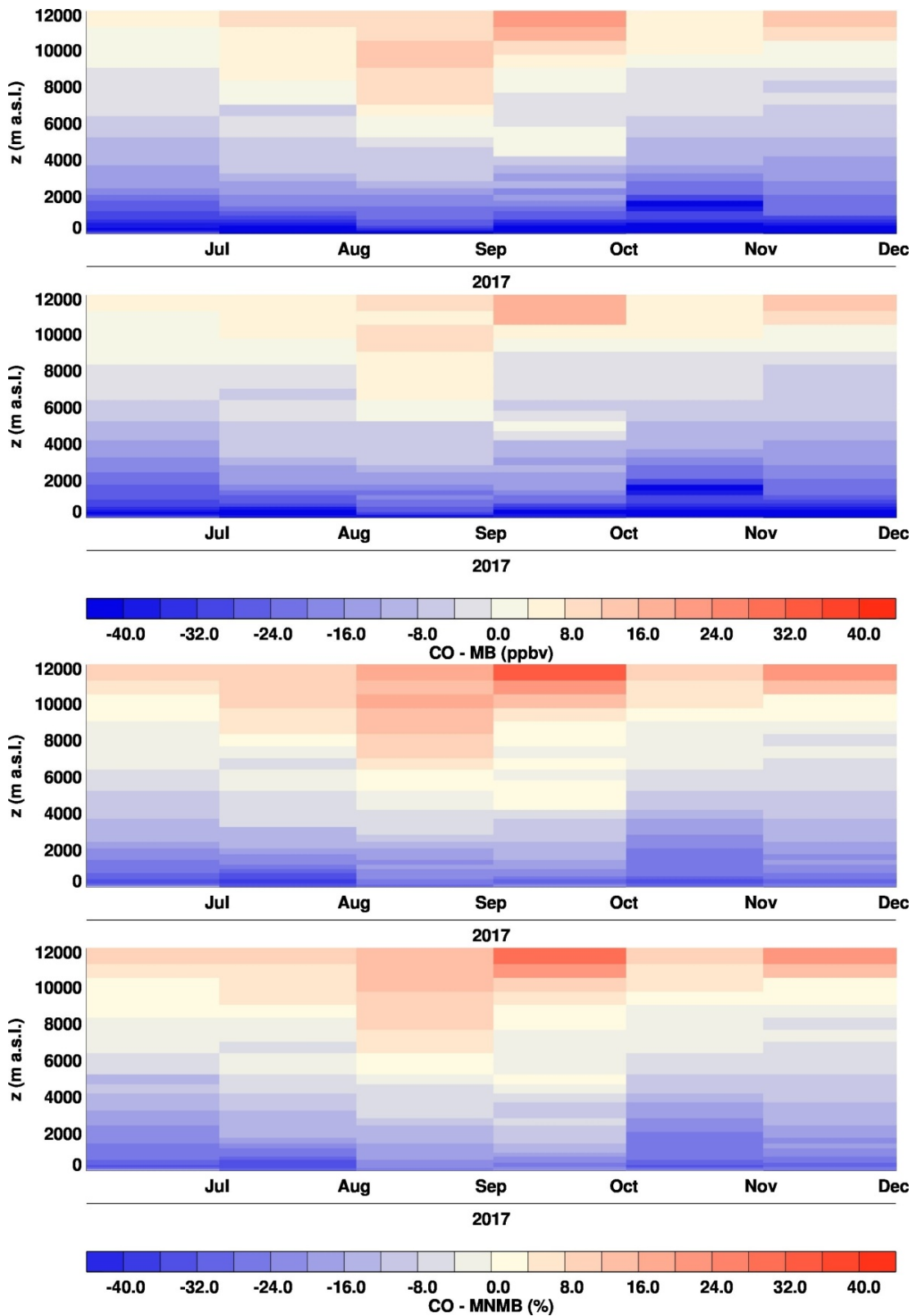
Figure 2.3.6: Time series of monthly analysis scores (MB in ppbv and NMB in %) for CO during the period June-November 2017. From top to bottom: Mean Bias (MB) for e-suite then for o-suite, Normalized Mean Bias (NMB) for e-suite then for o-suite.
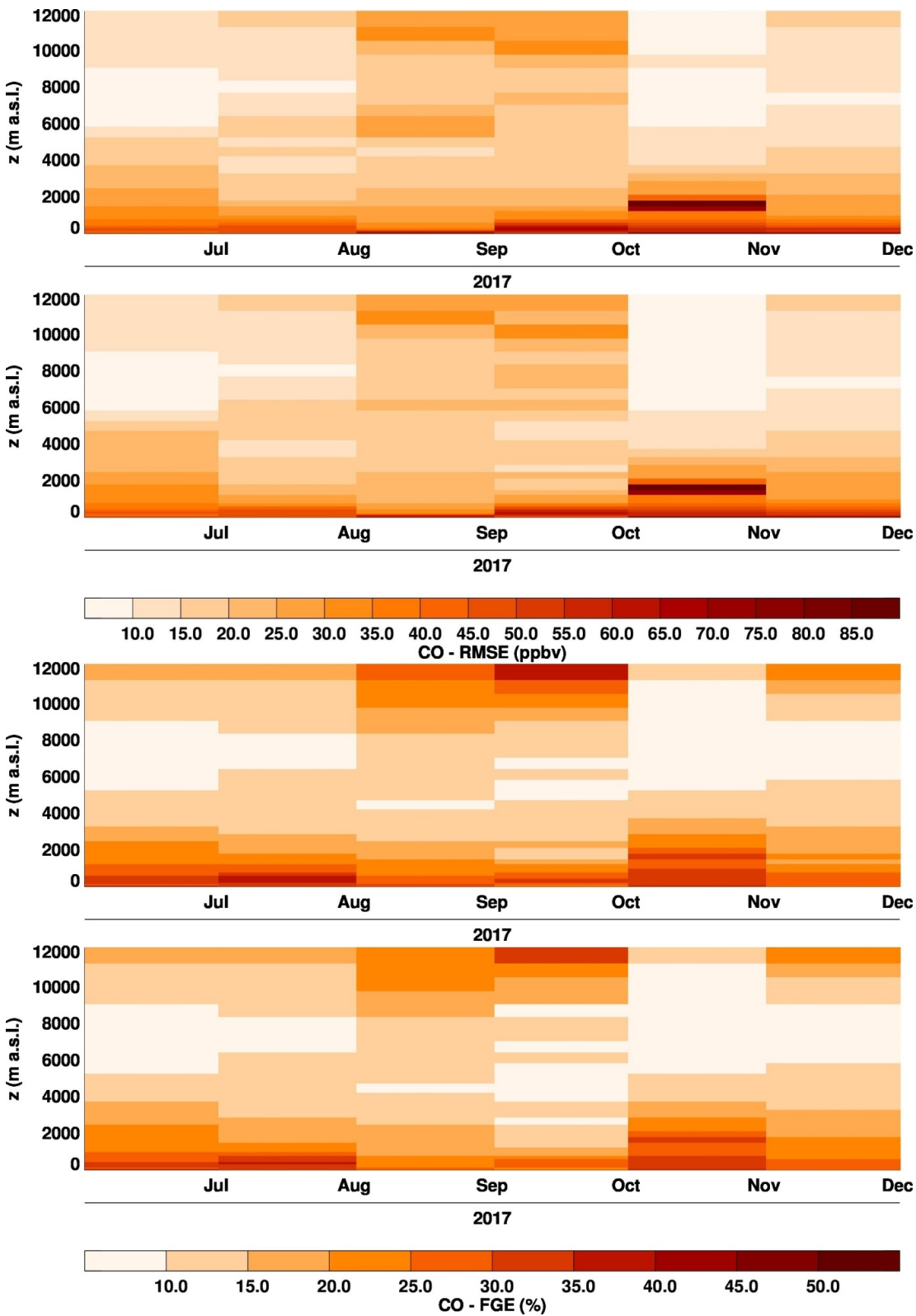
Figure 2.3.7: Time series of monthly analysis scores (RMSE in ppbv, and FGE in %) for ozone during the period June-November 2017. From top to bottom: Root Mean Square Error (RMSE) for e-suite then for o-suite, Fractional Gross Error (FGE) for e-suite then for o-suite.

2.3.3 Comparisons with MOPITTv6 and IASI CO data
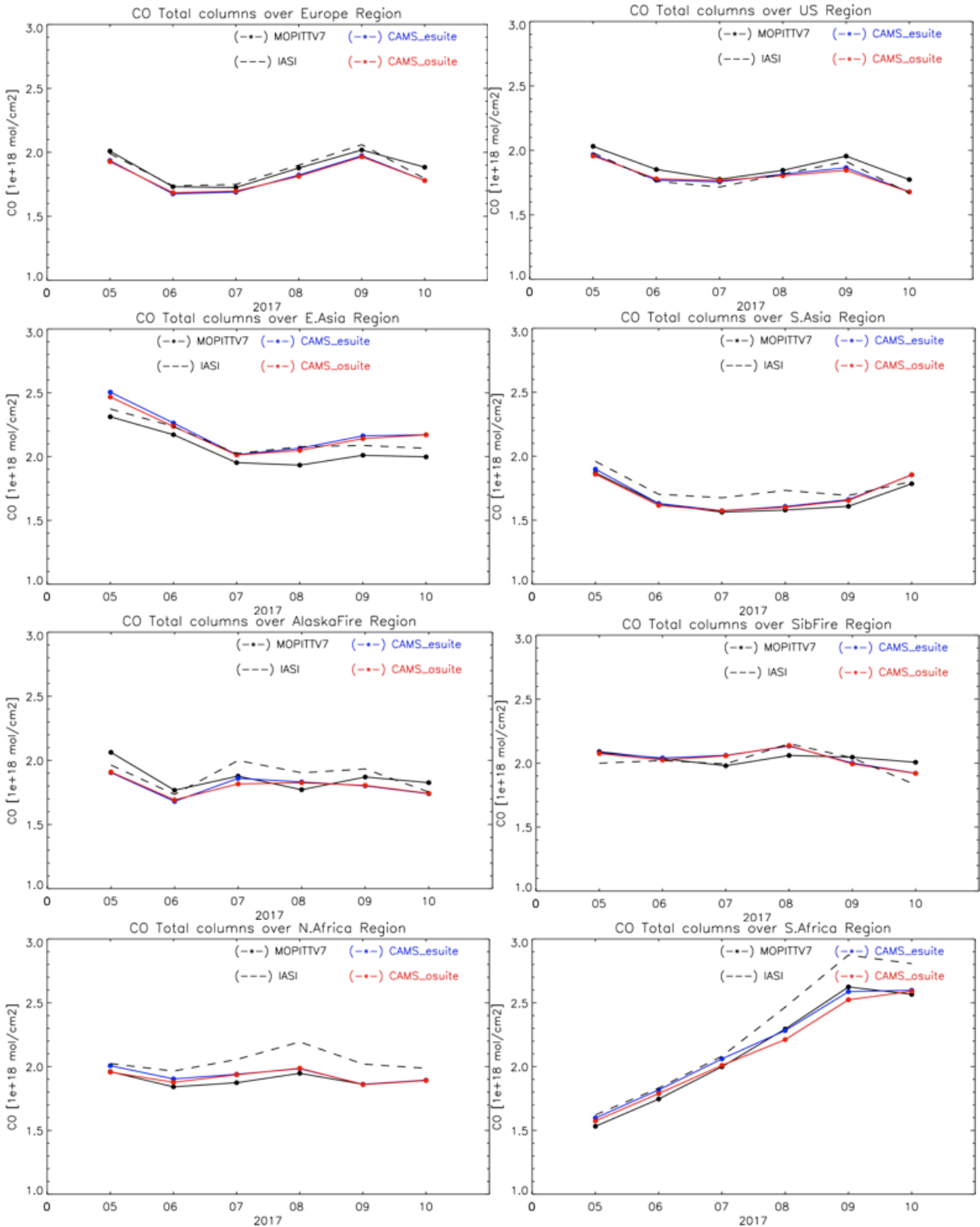
Fig.2.3.8. Time series of CO total columns for MOPITT v7 and IASI and the model simulations o-suite (red) and e-suite (blue) over selected regions for Mayuntil October 2017.
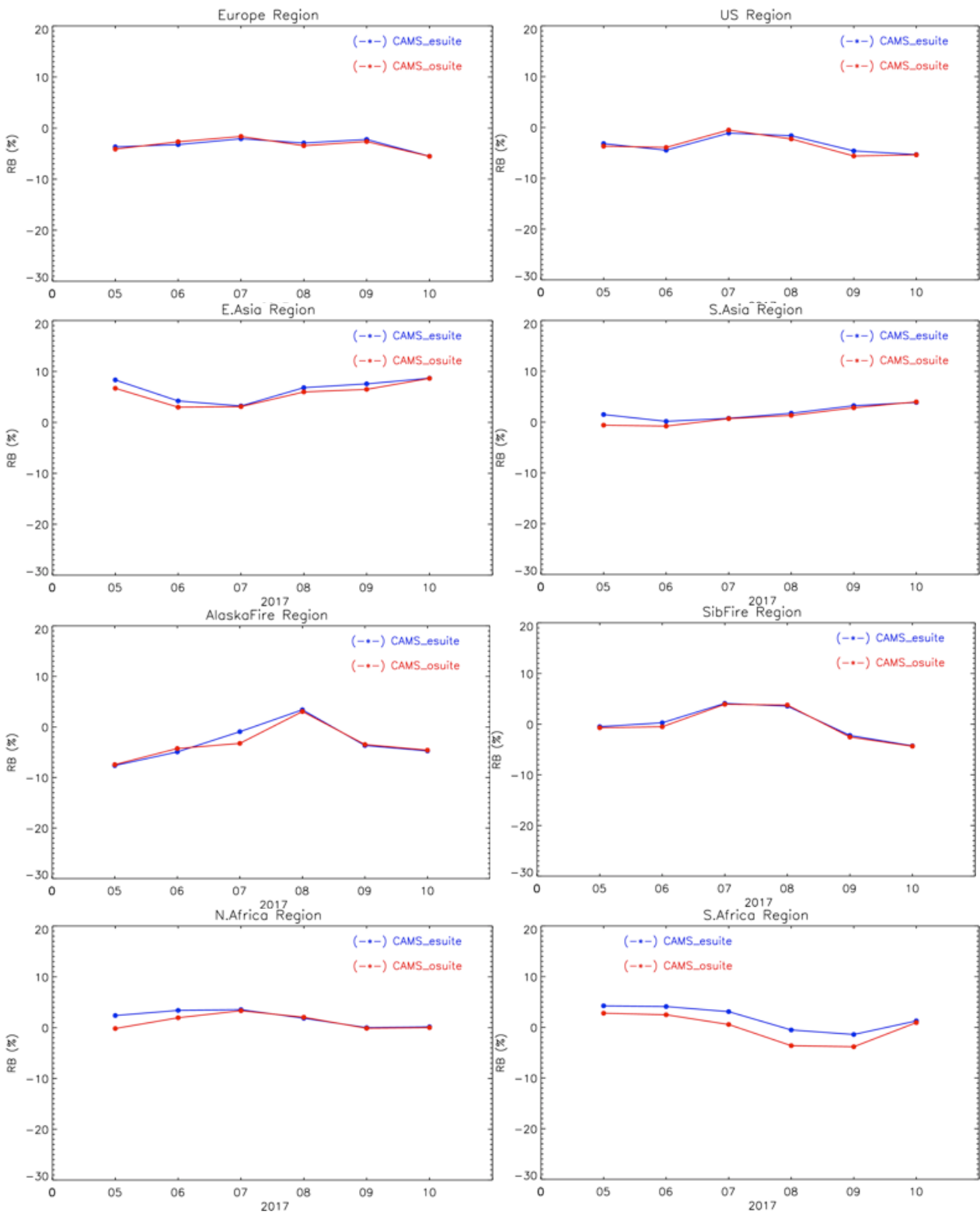
Fig.2.3.9: Bias in % of CAMS o-suite (red) and e-suite (blue) compared to MOPITTv7.
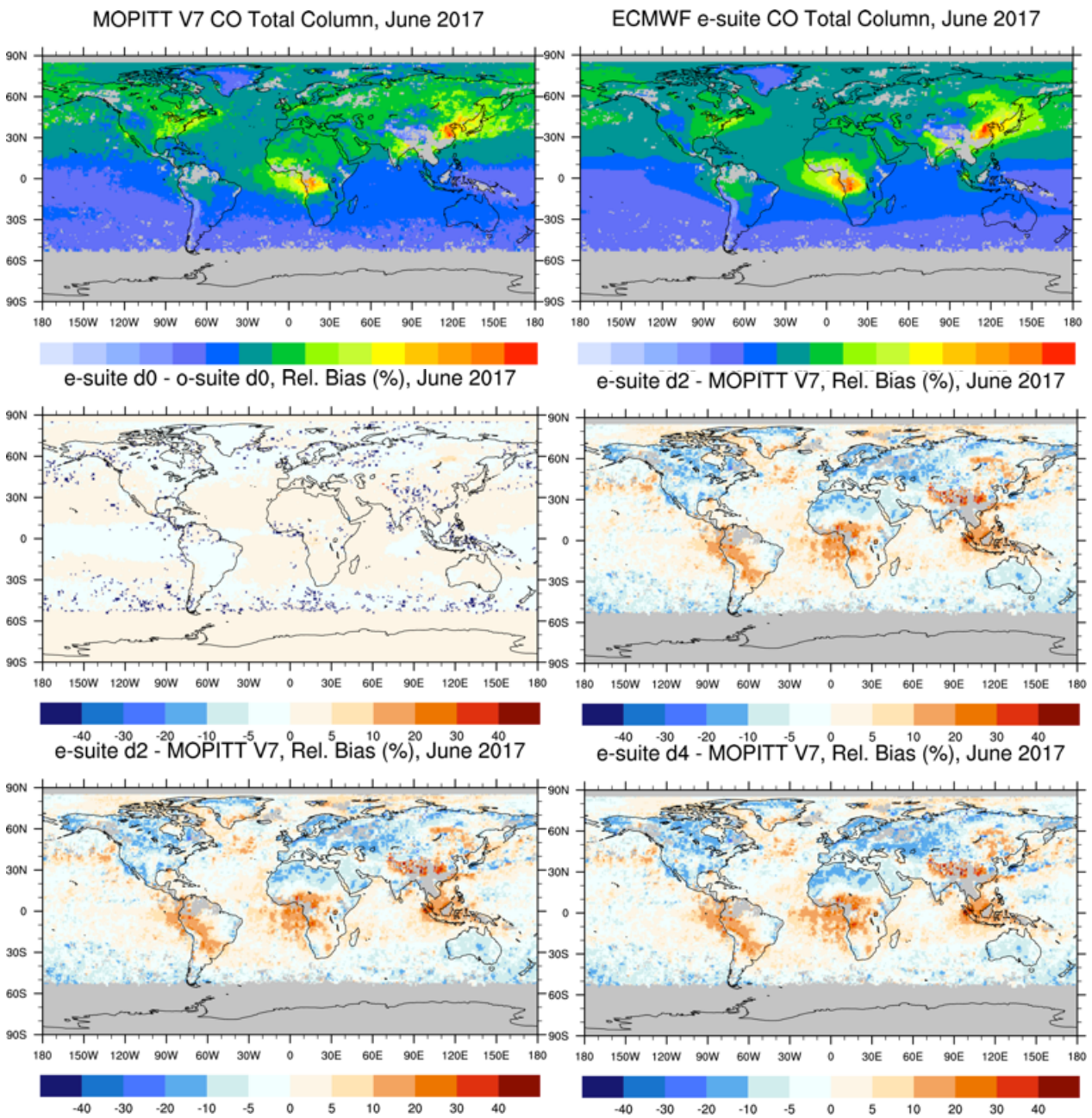
Figure 2.3.10: CO total columns for June 2017 from MOPITTv7 retrieval and the esuite simulation are shown in the upper most panel. The middle left panel shows the difference between osuite and esuite for June 2017, the middle right and the lower most panels show the difference between esuite d0, d2 and d4 and MOPITTv7 for June 2017

2.4 Nitrogen dioxide
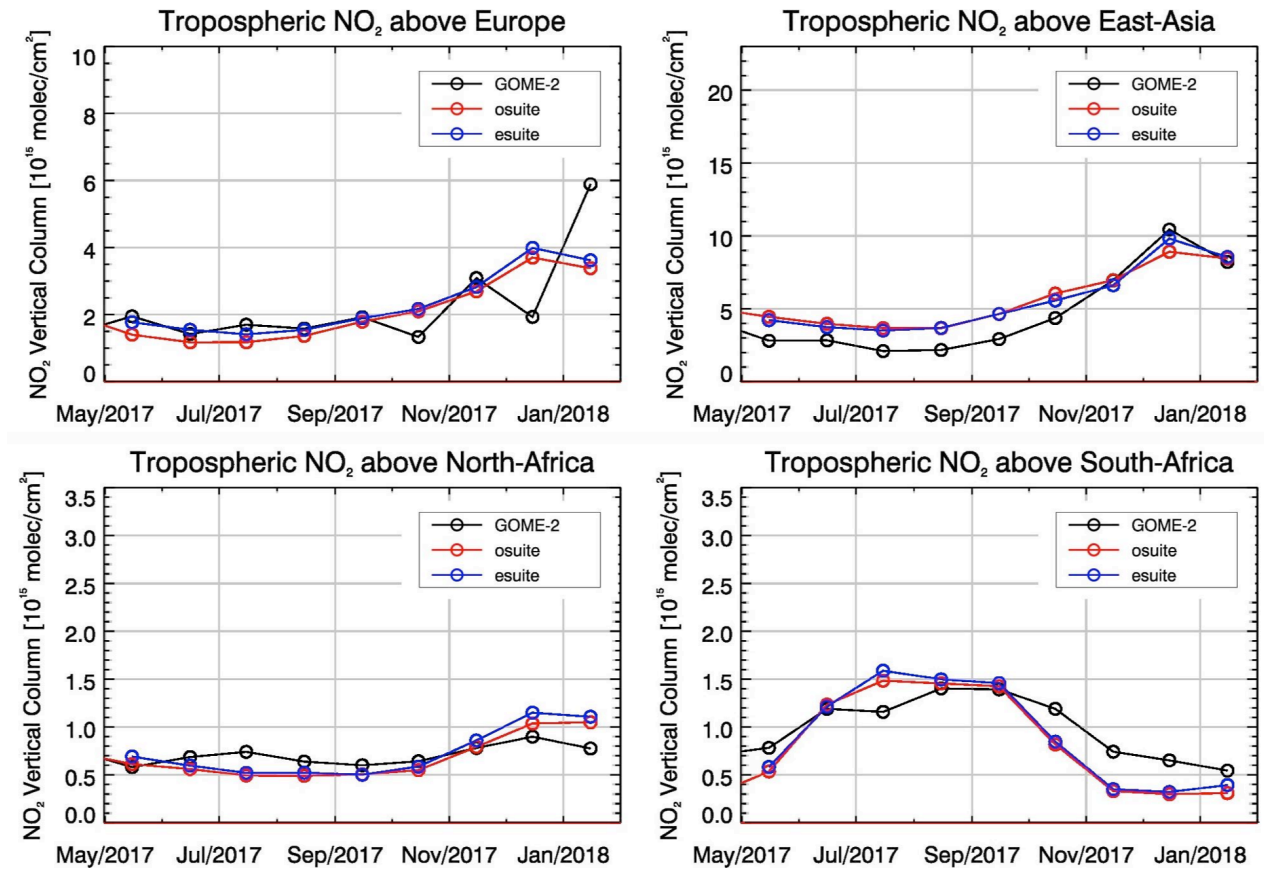
Figure 2.4.1: Time series of average tropospheric NO₂ columns [10¹⁵ molec cm⁻²] from GOME-2 compared to model results for different regions.
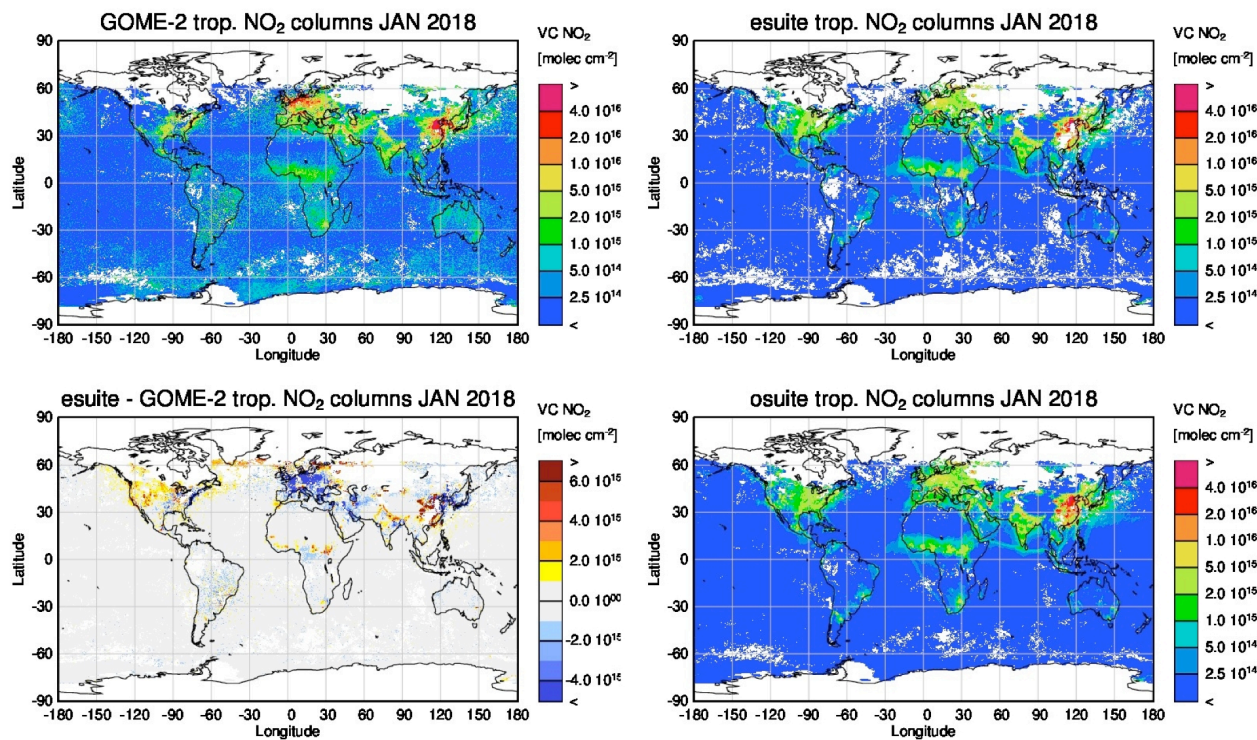
Figure 2.4.2: Monthly mean tropospheric NO₂ columns [molec cm⁻²] from GOME-2 compared to model runs for January 2018. The top row shows GOME-2 and esuite results, the lower one shows the difference between esuite and GOME-2 as well as osuite results. GOME-2 and model data were gridded to 0.4 degree resolution. Model data were treated with the same reference sector subtraction approach as the satellite data.

2.5 Formaldehyde (HCHO)
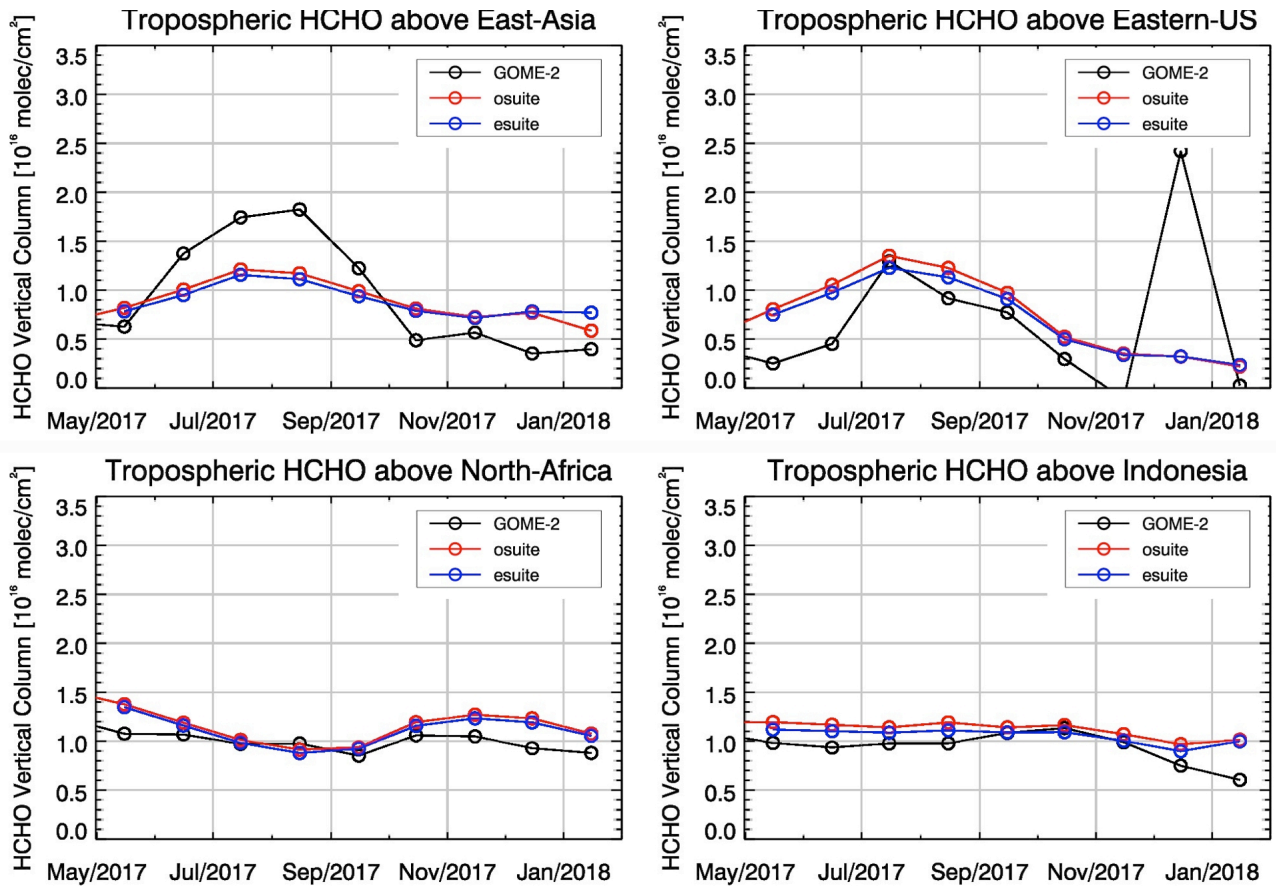
Figure 2.5.1: Time series of average tropospheric HCHO columns [10^{16} molec cm^{-2}] from GOME-2 compared to model results for different regions.
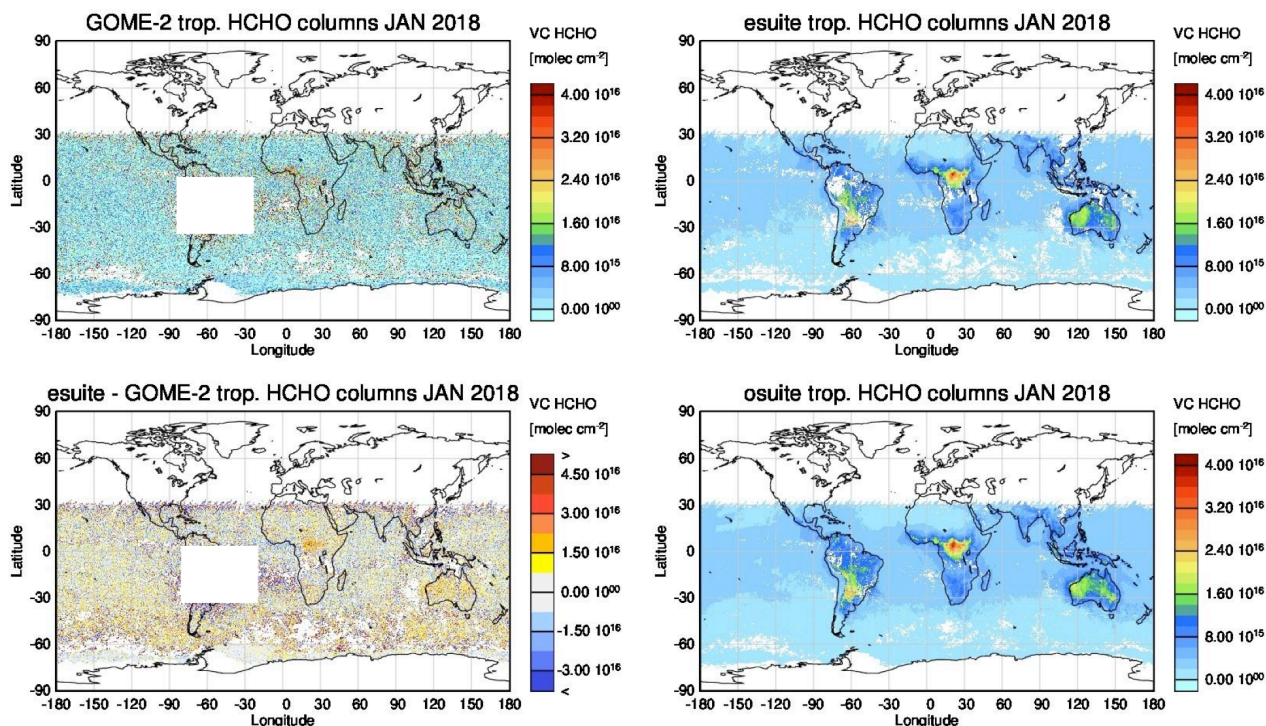
Figure 2.5.2: Monthly mean tropospheric HCHO columns [molec cm⁻²] from GOME-2 compared to model runs for January 2018. The top row shows GOME-2 and esuite results, the lower one shows the difference between esuite and GOME-2 as well as osuite results. GOME-2 and model data were gridded to 0.4 degree resolution. Model data were treated with the same reference sector subtraction approach as the satellite data. Satellite retrievals in the region of the South Atlantic Anomaly are not valid and therefore masked out (white box in panels on the left).
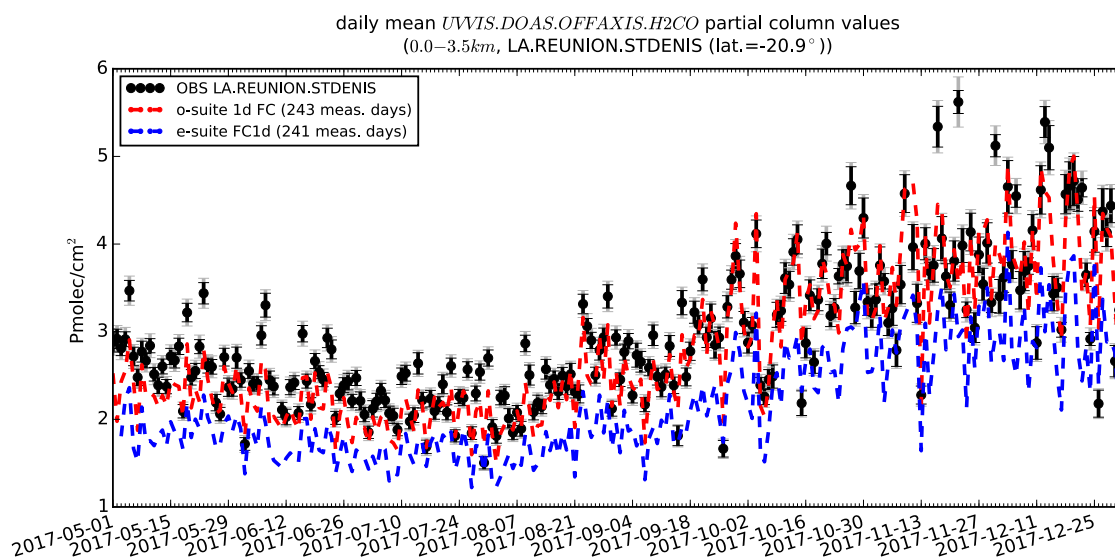
Figure 2.5.3: Daily mean values for 1d Forecast H2CO columns (0-3.5km) by the o-suite (red) and the e-suite run (blue) compared to NDACC UVVIS-DOAS OFFAXIS data at Reunion (21°S) for the period May 2017-December 2017. The bias of the -esuite increased.

2.6 Stratospheric ozone

2.6.1 Ozone sonde results
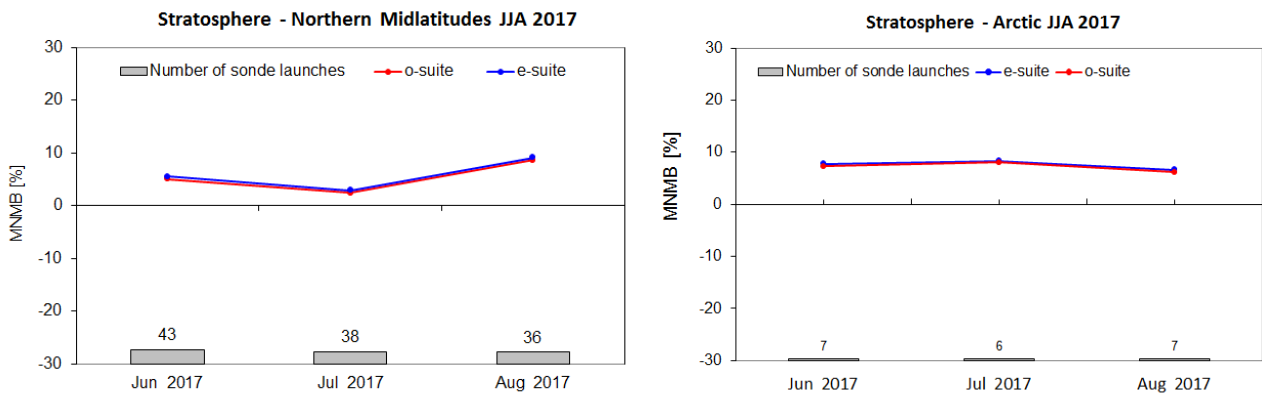
Fig. 2.6.1: MNMBs (%) of ozone in the stratosphere from the IFS model runs against aggregated sonde data over the Northern midlatiutdes (left) and the Arctic (right). The numbers indicate the amount of individual number of sondes.
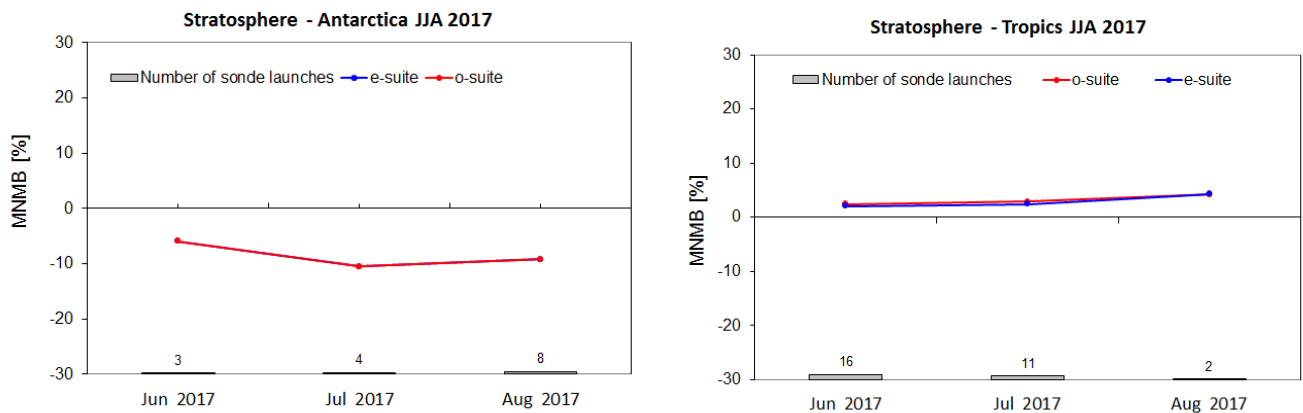

Fig. 2.6.2: MNMBs (%) of ozone in the stratosphere from the IFS model runs against aggregated sonde data over Antarctica (left) and the Tropics (right). The numbers indicate the amount of individual number of sondes.

2.6.2 Comparison with satellite observations
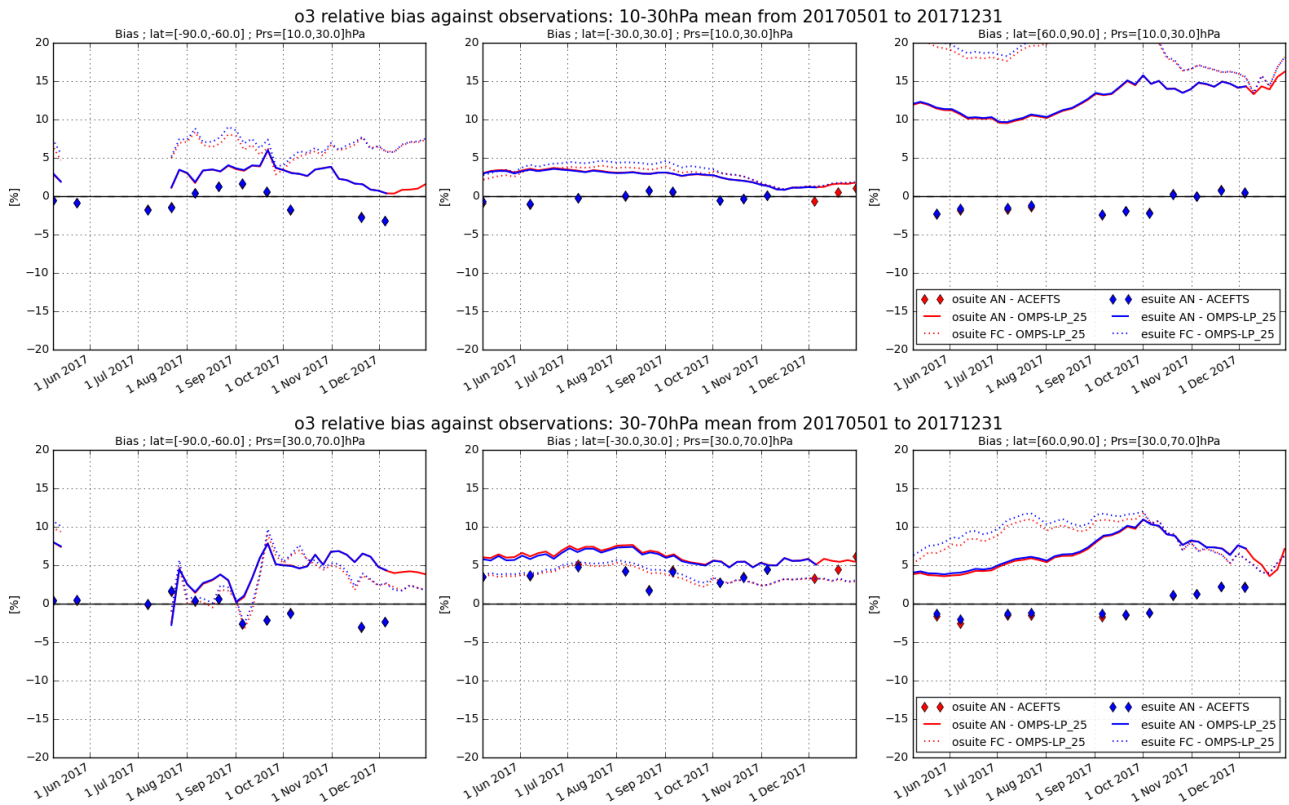
Figure 2.6.3: Mean normalized bias time series May-December 2017 of o-suite (red) analyses (solid) and 4th day forecast (dotted) and e-suite (blue) analyses (solid) and 4th day forecast (dotted) w.r.t. ACE-FTS (diamonds) and OMPS-LP (lines). Top panel: 10-30 hPa vertical range. Bottom panel: 30-70 hPa range.
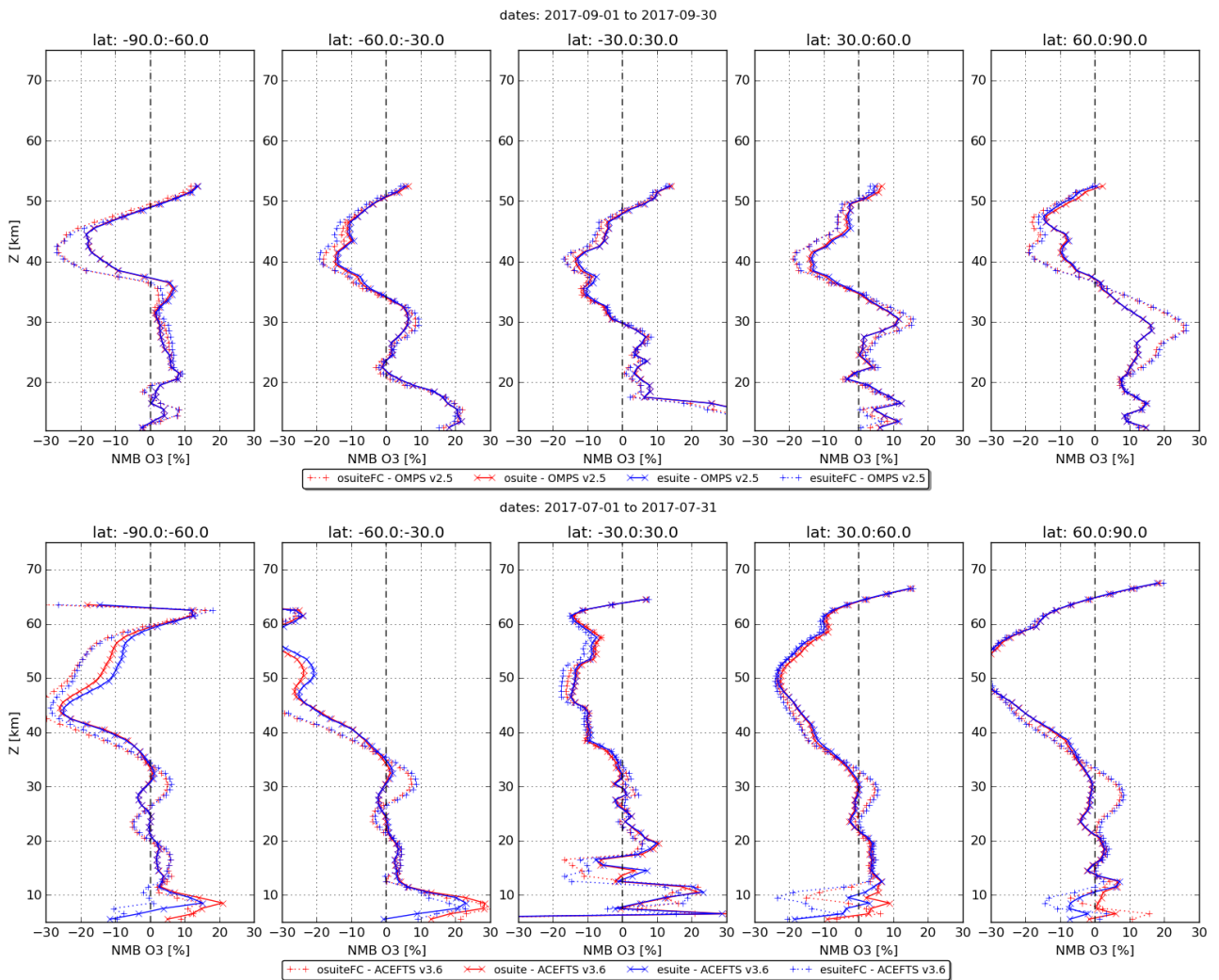
Figure 2.6.4: Mean normalized bias for ozone profiles of o-suite (red) analyses (solid) and 4th day forecast (dotted) and e-suite (blue) analyses (solid) and 4th day forecast (dotted) w.r.t. OMPS for the month of September 2017, and ACE-FTS for July 2017. The analyses of the o-suite and the e-suite are very close in the range 1hPa to 100hPa.
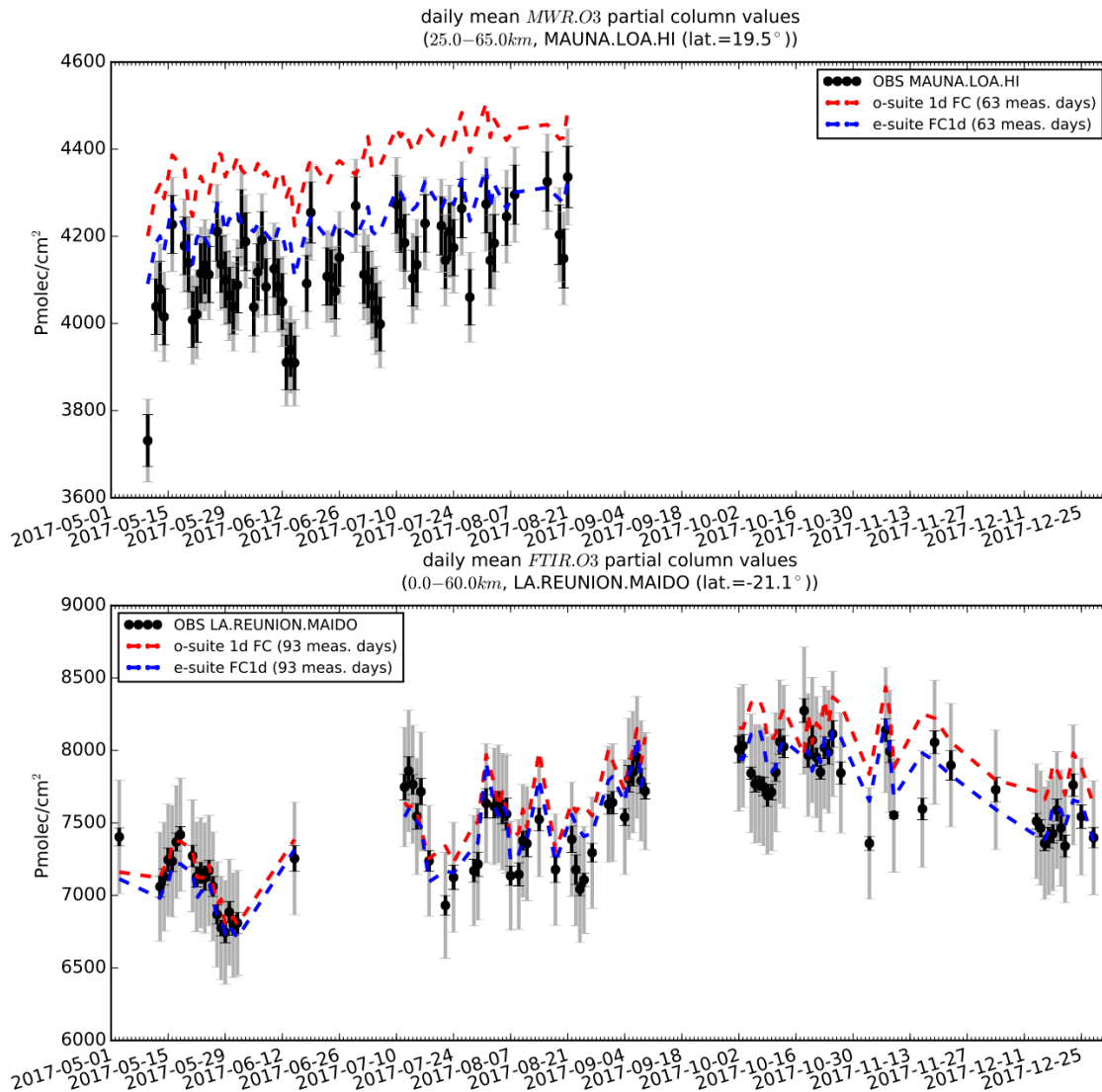
2.6.3 Comparison with NDACC observations

Fig. 2.6.5.: Daily mean values for 1d forecast for stratospheric O3 columns by the o-suite (red) and the e-suite run (blue) compared to NDACC MWR data at Mauna Loa (45°S, 19.5°N) and NDACC FTIR at Maido (21°S) for the period May 2017-December 2017. The bias of the e-suite 1d forecast is reduced and falls within the measurement uncertainty..
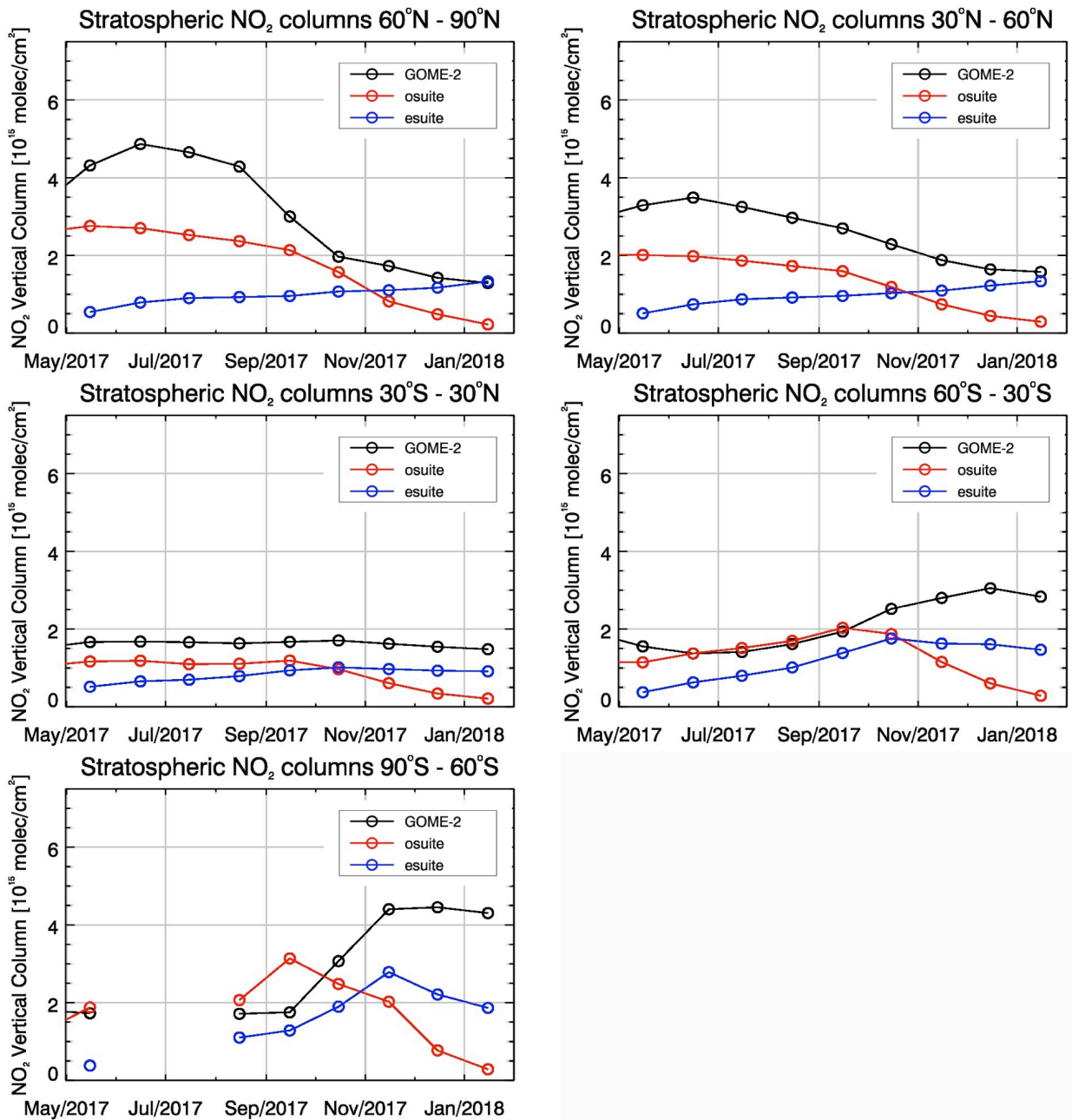
2.7 Stratospheric NO2

Figure 2.7.1: Time series of average stratospheric NO_2 columns [10^{15} molec cm-2] from GOME-2 compared to model results for different latitude bands.
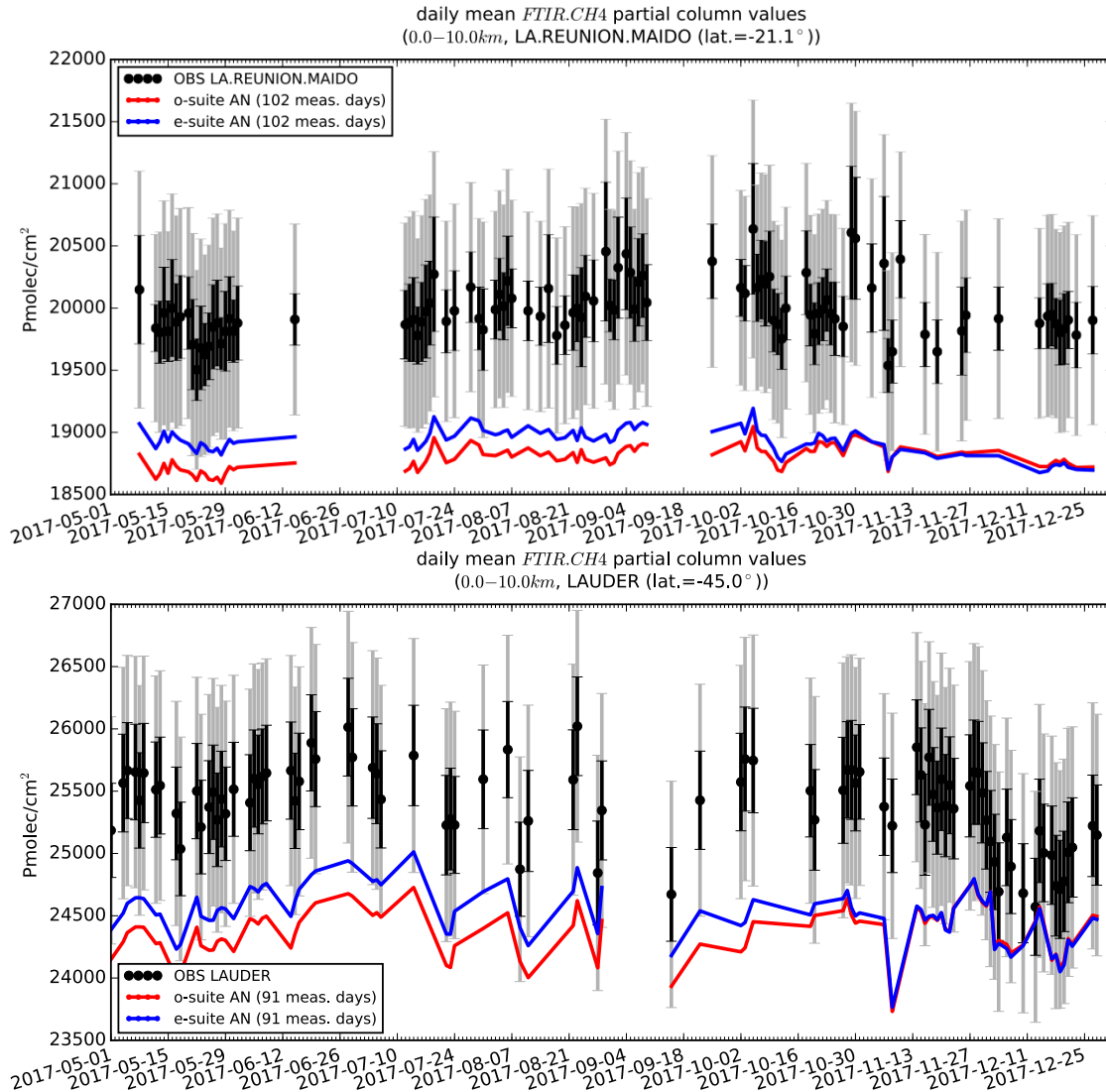
2.8 Methane

Fig. 2.8.1: Daily mean values for AN CH₄ columns (0-10km) by the o-suite (red) and the e-suite run (blue) compared to NDACC FTIR data at Maido (21°S) and Lauder (45°S) for the period May 2017-December 2017. The bias of the e-suite is reduced and now falls within the measurement uncertainty. The diference between the o- and e-suite seems to vanish near the end of 2017.

3. References

Benedetti, A., J.-J. Morcrette, O. Boucher, A. Dethof, R. J. Engelen, M. Fisher, H. Flentjes, N. Huneeus, L. Jones, J. W. Kaiser, S. Kinne, A. Mangold, M. Razinger, A. J. Simmons, M. Suttie, and the GEMS-AER team: Aerosol analysis and forecast in the ECMWF Integrated Forecast System. Part II : Data assimilation, J. Geophys. Res., 114, D13205, doi:10.1029/2008JD011115, 2009.

Cariolle, D. and Teyssèdre, H.: A revised linear ozone photochemistry parameterization for use in transport and general circulation models: multi-annual simulations, Atmos. Chem. Phys., 7, 2183-2196, doi:10.5194/acp-7-2183-2007, 2007.

Dee, D. P. and S. Uppala, Variational bias correction of satellite radiance data in the ERA-Interim reanalysis. Quart. J. Roy. Meteor. Soc.,135, 1830-1841, 2009.

Eskes, H., Huijnen, V., Arola, A., Benedictow, A., Blechschmidt, A.-M., Botek, E., Boucher, O., Bouarar, I., Chabrillat, S., Cuevas, E., Engelen, R., Flentje, H., Gaudel, A., Griesfeller, J., Jones, L., Kapsomenakis, J., Katragkou, E., Kinne, S., Langerock, B., Razinger, M., Richter, A., Schultz, M., Schulz, M., Sudarchikova, N., Thouret, V., Vrekoussis, M., Wagner, A., and Zerefos, C.: Validation of reactive gases and aerosols in the MACC global analysis and forecast system, Geosci. Model Dev., 8, 3523-3543, doi:10.5194/gmd-8-3523-2015, 2015.

Douros, J., S. Basart, A. Benedictow, A.-M. Blechschmidt, S. Chabrillat, Y. Christophe, H. Clark, E. Cuevas, H.J. Eskes, H. Flentje, K. M. Hansen, J. Kapsomenakis, B. Langerock, K. Petersen, M. Ramonet, A. Richter, M. Schulz, A. Wagner, T. Warneke, C. Zerefos, Observations characterisation and validation methods document, Copernicus Atmosphere Monitoring Service (CAMS) report, CAMS84_2015SC2_D.84.8.1.1-2017_observations_v2.pdf, October 2017. Available from: http://atmosphere.copernicus.eu/user-support/validation/verification-global-services.

H.J. Eskes, A. Wagner, M. Schulz, Y. Christophe, M. Ramonet, S. Basart, A. Benedictow, Y. Bennouna, A.-M. Blechschmidt, S. Chabrillat, H. Clark, E. Cuevas, H. Flentje, K.M. Hansen, U. Im, J. Kapsomenakis, B. Langerock, K. PetersEN, A. Richter, N. Sudarchikova, V. Thouret, T. Warneke, C. Zerefos, Validation report of the CAMS near-real-time global atmospheric composition service: Period September-November 2017, Copernicus Atmosphere Monitoring Service (CAMS) report, CAMS84_2015SC3_D84.1.1.10_2017SON_v1.pdf, February 2018.

Eskes, H.J., A. Wagner, M. Schulz, Y. Christophe, M. Ramonet, S. Basart, A. Benedictow, A.-M. Blechschmidt, S. Chabrillat, H. Clark, E. Cuevas, H. Flentje, K.M. Hansen, U. Im, J. Kapsomenakis, B. Langerock, K. PetersEN, A. Richter, N. Sudarchikova, V. Thouret, T. Warneke, C. Zerefos, Validation report of the CAMS near-real-time global atmospheric composition service: December 2016 - February 2017, Copernicus Atmosphere Monitoring Service (CAMS) report, CAMS84_2015SC2_D84.1.1.7_2017DJF_v1.pdf, May 2017.

Flemming, J., Huijnen, V., Arteta, J., Bechtold, P., Beljaars, A., Blechschmidt, A.-M., Diamantakis, M., Engelen, R. J., Gaudel, A., Inness, A., Jones, L., Josse, B., Katragkou, E., Marecal, V., Peuch, V.-H., Richter, A., Schultz, M. G., Stein, O., and Tsikerdekis, A.: Tropospheric chemistry in the Integrated Forecasting System of ECMWF, Geosci. Model Dev., 8, 975-1003, doi:10.5194/gmd-8-975-2015, 2015.

Granier, C. et al.: Evolution of anthropogenic and biomass burning emissions of air pollutants at global and regional scales during the 1980–2010 period. Climatic Change (109), 2011.

Huijnen, V., et al.: The global chemistry transport model TM5: description and evaluation of the tropospheric chemistry version 3.0, Geosci. Model Dev., 3, 445-473, doi:10.5194/gmd-3-445-2010, 2010.

Inness, A., Blechschmidt, A.-M., Bouarar, I., Chabrillat, S., Crepulja, M., Engelen, R. J., Eskes, H., Flemming, J., Gaudel, A., Hendrick, F., Huijnen, V., Jones, L., Kapsomenakis, J., Katragkou, E., Keppens, A., Langerock, B., de Mazière, M., Melas, D., Parrington, M., Peuch, V. H., Razinger, M., Richter, A., Schultz, M. G., Suttie, M., Thouret, V., Vrekoussis, M., Wagner, A., and Zerefos, C.: Data assimilation of satellite-retrieved ozone, carbon monoxide and nitrogen dioxide with ECMWF's Composition-IFS, Atmos. Chem. Phys., 15, 5275-5303, doi:10.5194/acp-15-5275-2015, 2015.

Kaiser, J. W., Heil, A., Andreae, M. O., Benedetti, A., Chubarova, N., Jones, L., Morcrette, J.-J., Razinger, M., Schultz, M. G., Suttie, M., and van der Werf, G. R.: Biomass burning emissions estimated with a global fire assimilation system based on observed fire radiative power, Biogeosciences, 9, 527-554, doi:10.5194/bg-9-527-2012, 2012.

Morcrette, J.-J., O. Boucher, L. Jones, D. Salmond, P. Bechtold, A. Beljaars, A. Benedetti, A. Bonet, J. W. Kaiser, M. Razinger, M. Schulz, S. Serrar, A. J. Simmons, M. Sofiev, M. Suttie, A. M. Tompkins, and A. Untch: Aerosol analysis and forecast in the ECMWF Integrated Forecast System. Part I: Forward modelling, J. Geophys. Res., 114, D06206, doi:10.1029/2008JD011235, 2009.

Annex 1: Acknowledgements for measurements used

We wish to acknowledge the provision of NRT GAW observational data by: Institute of Atmospheric Sciences and Climate (ISAC) of the Italian National Research Council (CNR), South African Weather Service, National Centre for Atmospheric Science (NCAS, Cape Verde), National Air Pollution Monitoring Network (NABEL) (Federal Office for the Environment FOEN and Swiss Federal Laboratories for Materials Testing and Research EMPA), Atmospheric Environment Division Global Environment and Marine Department Japan Meteorological Agency, Chinese Academy of Meteorological Sciences (CAMS), Alfred Wegener Institut, Umweltbundesamt (Austria), National Meteorological Service (Argentina), Umweltbundesamt (UBA, Germany)

We are grateful to the numerous operators of the Aeronet network and to the central data processing facility at NASA Goddard Space Flight Center for providing the NRT sun photometer data, especially Ilya Slutker and Brent Holben for sending the data.

The authors thank to all researchers, data providers and collaborators of the World Meteorological Organization's Sand and Dust Storm Warning Advisory and Assessment System (WMO SDS-WAS) for Northern Africa, Middle East and Europe (NAMEE) Regional Node. Also special thank to Canary Government as well as AERONET, MODIS, U.K. Met Office MSG, MSG Eumetsat and EOSDIS World Viewer principal investigators and scientists for establishing and maintaining data used in the activities of the WMO SDS-WAS NAMEE Regional Center (http://sds-was.aemet.es/).

We wish to acknowledge the provision of ozone sonde data by the World Ozone and Ultraviolet Radiation Data Centre established at EC in Toronto (http://woudc.org), by the Data Host Facility of the Network for the Detection of Atmospheric Composition Change established at NOAA (http://ndacc.org), by the Norwegian Institute for Air Research and by the National Aeronautics and Space Administration (NASA).

We wish to thank the NDACC investigators for the provision of observations at Ny Alesund, Bern, Jungfraujoch, Izaña, Xianghe, Harestua, Reunion Maido, Uccle, Hohenpeissen, Mauna Loa, Lauder and Haute Provence. Special thanks to the data providers at Ny-Alesund, Bern and Uccle for their support of the Arctic ozone depletion case study.

The authors acknowledge the NOAA Earth System Research Laboratory (ESRL) Global Monitoring Division (GMD) for the provision of ground based ozone concentrations.

The MOPITT CO data were obtained from the NASA Langley Research Center ASDC. We acknowledge the LATMOS IASI group for providing IASI CO data.

SCIAMACHY lv1 radiances were provided to IUP-UB by ESA through DLR/DFD.

GOME-2 lv1 radiances were provided to IUP-UB by EUMETSAT.

The authors acknowledge Environment and Climate Change Canada for the provision of Alert ozone data and Sara Crepinsek – NOAA for the provision of Tiksi ozone data. Surface ozone data from the Villum Research Station, Station Nord (VRS) was financially supported by "The Danish

Copernicus Atmosphere Monitoring Service